

# From the Top: Surface-derived Carbon Fuels Greenhouse Gas Production at Depth in a Neotropical Peatland

Alexandra Hedgpeth<sup>1,2</sup>, Alison M. Hoyt<sup>3</sup>, Kyle Cavanaugh<sup>1</sup>, Karis J. McFarlane<sup>2\*</sup>, Daniela F. Cusack<sup>1,4,5\*</sup>

5 <sup>1</sup>Geography Department, University of California Los Angeles, Los Angeles, 94143, USA

<sup>2</sup>Lawrence Livermore National Laboratory, Livermore, 94550, USA

<sup>3</sup>Department of Earth System Science, Stanford University, Stanford, 94305, USA

<sup>4</sup>Department of Ecosystem Science & Sustainability, Colorado State University, Fort Collins, 80523, USA

<sup>5</sup>Smithsonian Tropical Research Institute, Balboa, Ancon, Republic of Panama, 0843-03092

10

★ These authors contributed equally to this work

*Correspondence:* Alexandra Hedgpeth ([hedgpea10@g.ucla.edu](mailto:hedgpea10@g.ucla.edu))

## Abstract.

15 Tropical peatlands play an important role in global carbon (C) cycling but little is known about factors driving carbon dioxide (CO<sub>2</sub>) and methane (CH<sub>4</sub>) emissions from these ecosystems, especially production in deeper soils. This study aimed to identify source material and processes regulating C emissions originating deep in three Neotropical peatland sites on the Caribbean coast of Panama. We hypothesized that: 1) surface derived organic matter transported down the soil profile is the primary C source for respiration products at depth; 2) high lignin content results in hydrogenotrophic methanogenesis as the dominant  
20 CH<sub>4</sub> production pathway throughout the profile, which relies on organic matter fermentation rather than carbon dioxide. We used radiocarbon isotopes to determine whether CO<sub>2</sub> and CH<sub>4</sub> at depth are produced from modern substrates or ancient deep peat, and we used stable C isotopes to identify the dominant CH<sub>4</sub> production pathway. Peat organic chemistry was characterized using <sup>13</sup>C solid state nuclear magnetic resonance spectroscopy (<sup>13</sup>C-NMR). We found that deep peat respiration products had radiocarbon signatures that were more similar to surface dissolved organic C (DOC) than deep solid peat, even though the peat  
25 chemistry remained relatively stable from the surface to the deeper layers. These results indicate that surface derived organic matter was the dominant source for gas production at depth in this peatland, likely because of vertical transport of DOC from the surface to depth. Lignin, which was the most abundant compound (55-70% of C), increased with depth across these sites, whereas other C compounds like carbohydrates did not vary with depth. These results suggest that there is no preferential decomposition of carbohydrates, but preferential retention of lignin. Stable isotope signatures of respiration products indicated  
30 that hydrogenotrophic rather than acetoclastic methanogenesis was the dominant production pathway of CH<sub>4</sub> throughout the peat profile, suggesting dominance of respiration rather than fermentation for fuelling methanogenesis. These results show that deep C in tropical peatlands does not contribute greatly to surface fluxes of carbon dioxide, with compounds like lignin preferentially retained. This protection of deep C helps explain how peatland C is retained over thousands of years, and points to the vulnerability of this C should anaerobic conditions in these wet ecosystems change.

## 35 **1 Introduction**

Climate change is expected to disturb hydrological cycles in the tropics, with changes in rainfall regimes already observed for many tropical regions (Kharin et al. 2007, Feng et al. 2013, Magrin et al. 2014, Duffy et al. 2015, Chadwick et al. 2016, Barkhordarian et al. 2019). Changes in rainfall are of particular relevance to the storage of the 70 – 130 Gt of organic carbon (OC) stored in tropical peatland soils under anaerobic conditions, which could be under threat of rapid mineralization if rainfall declines and aerobic conditions emerge (Girkin et al., 2022; Loisel et al., 2021). Tropical peatlands store the largest pool of vulnerable and irrecoverable C of any ecosystem type, and this pool is sequestered over thousands of years (Goldstein et al., 2020; Noon et al., 2021). Despite their importance, tropical peatlands are logistically challenging environments to work in and are understudied compared to their northern counterparts, making tropical peatlands underrepresented in global C inventories (Ribeiro et al., 2021).

Peatlands sequester C as they build vertically with the oldest deposits at the base and less decomposed younger material accumulating at the surface (Clymo et al., 1998; Ingram, 1987). Despite temperatures ideal for microbial activity, the buildup of organic matter is possible because rates of primary production in the tropics exceed decomposition rates, which are low because peatland water tables are high (Nottingham et al., 2019; Page et al., 2011). Thus, deep peat is comprised of minimally processed plant material from the surface that accumulates due to anaerobic conditions, creating a globally significant buildup of C over time that could be metabolized if conditions became more favorable for decomposition (Hoyos-Santillan et al., 2019; Kettridge et al., 2015; Wilson et al., 2021). However, this age-depth relationship is not as straightforward in the tropics as in northern peatlands, because tropical peatland microtopography shows higher variability due to increased vegetation diversity and size, and forest disturbance can have dramatic effects on peat accumulation patterns (Dommain et al., 2015; Girkin et al., 2019). The dominant vegetation that acts as the stabilizing structure in early peat development, as well as the vegetation that serves as the biological origin of the peat itself, is also different in northern and tropical peatlands, leading to differences in peatland development, organic chemistry, and accumulation patterns between these two regions (United Nations Environment Programme et al., 2008).

Under current conditions, there is considerable variation in C emissions across tropical wetland systems (Farmer et al., 2011; Fritts, 2022), but some relationships have been generally characterized. It is mostly accepted that water table depth (Cobb et al., 2017; Hoyos-Santillan et al., 2019; Hoyt et al., 2019), temperature (Girkin et al., 2020; Hirano et al., 2009; Jauhiainen et al., 2014), substrate availability, and associated links with the dominant vegetation type (Upton et al., 2018; Wright et al., 2011, 2013), are strong controls on atmospheric emissions from tropical peatlands. Furthermore, surface vegetation plays an important role in the release of C by several processes, including being the biological origin of the peat matrix, which is composed primarily of lignin rich fibrous material in woody tropical peatlands, and determining labile C inputs in the form of decomposing plant tissues or root exudates (Girkin et al., 2018b; Lampela et al., 2014; Osaki et al., 2021). The majority of studies conducted in tropical peatlands have focused on the top 30 cm of the peat column; these depths are not only more accessible and easier to measure, but they are assumed to contribute the majority of emissions (Dhandapani et al.,

2022; Jauhiainen et al., 2005; Sjögersten et al., 2011). However, it is not known if the above drivers are mainly restricted to the surface, or if these processes influence CO<sub>2</sub> and CH<sub>4</sub> production deeper within the peat profile.

70 In many peatlands, microbial respiration across the soil profile can be supported by multiple C sources, and it is possible to use the radiocarbon signature of C respired from peatlands to partition sources into modern/surface dissolved OC (DOC) transported down the soil profile, versus older/buried solid C (Chanton et al., 2008; Hoyos-Santillan et al., 2016). Modern DOC, derived from surface vegetation, root exudates, and other recently photosynthesized organic matter, has a signature that is enriched in  $\Delta^{14}\text{C}$ . The existing peat and DOC from *in situ* decomposition of that deep peat, would have depleted radiocarbon  
75 signatures compared to the modern DOC (Girkin et al., 2018b; Wilson et al., 2016).

There have been several studies exploring the source of DOC used by microbes for respiration within peat soils. Most studies were from northern peatlands, and determined that respiration products were intermediate in their radiocarbon activity between newer surface DOC and *in situ* older C in peat (Aravena et al., 1993; Chanton et al., 1995, 2008; Charman et al., 1999; Clymo and Bryant, 2008; Elizabeth Corbett et al., 2013). Fewer studies have reported that respiration products are more similar  
80 to modern DOC radiocarbon signatures, demonstrating dominant use of surface DOC in deep peat gas production (Wilson et al., 2021). There is limited data from tropical peatlands, but two previous studies from the tropics have contrasting results; one shows intermediate respiration products (i.e., produced by mixed sources) in a tropical peatland in Borneo (Hoyt, 2014), and another shows modern, surface-derived inputs are the dominant source in sites across the Pastaza-Marañón basin in Peru (Hoyt et al., 2020). Potential explanations for this variable source contribution in tropical peatlands include differences in hydrology  
85 across sites, as well as the difference in dominant vegetation across the tropics. Biological origin can influence the chemistry and bioavailability of both modern DOC inputs and the resulting older peat (Dhandapani et al., 2023; Gandois et al., 2014), which could contribute to the different results reported for these two tropical peatlands with distinct surface vegetation.

Methanogenesis is an important pathway of decomposition in wetland systems. Acetoclastic methanogenesis is associated with acetate fermentation and the production of CH<sub>4</sub> from relatively labile organic compounds, while hydrogenotrophic  
90 methanogenesis is associated with CO<sub>2</sub> reduction, and can be supplied by the decomposition of more complex organic matter, with this second pathway less energetically favourable to microbes (Kotsyurbenko et al., 2004; Sugimoto and Wada, 1993). Metabolically, acetoclastic methanogenesis is more energetically favourable (i.e. more potential energy released), more efficient in CH<sub>4</sub> production, and generally results in higher rates of CH<sub>4</sub> production compared to hydrogenotrophic methanogenesis (Kotsyurbenko et al., 2004; Liebner et al., 2015). Shifts in CH<sub>4</sub> production pathways between acetoclastic  
95 methanogenesis and hydrogenotrophic methanogenesis occur depending on substrate availability, with acetoclastic favoured if fermentation products are available, as have been seen with depth in northern wetlands (Chanton et al., 2008; Corbett et al., 2013; Hornibrook et al., 2000). Changes in the availability of labile materials throughout the peat profile, even at depths of 2 meters, may be crucial not only for supplying the C substrate for CO<sub>2</sub> and CH<sub>4</sub> production, but also for influencing the mechanisms and quantities of CH<sub>4</sub> generated (Moore et al., 2013; Sun et al., 2012).

100 This study explored sources of soil surface C emissions, CH<sub>4</sub> production pathways, and organic carbon chemistry of peat in three sites in a Neotropical peatland in Panama. Previous work suggested that subsurface peat may contribute

substantially to net CO<sub>2</sub> and CH<sub>4</sub> flux from this peatland, but the source of C for these emissions was unclear (Wright et al., 2011). We used a combination of stable and radioisotope signatures of CO<sub>2</sub> and CH<sub>4</sub>, and <sup>13</sup>C solid state nuclear magnetic resonance spectroscopy (<sup>13</sup>C-NMR) characterization of peat soils, to identify the sources of the C gases produced in subsurface  
105 (>30 cm) peat. We hypothesized that: H1) surface-derived DOC is the primary C source for microbial respiration products at depth, where solid peat is more chemically complex and protected against decomposition. For this hypothesis, we predicted that deep solid peat would have a higher decomposition index compared with surface peat. H2) Hydrogenotrophic methanogenesis is the dominant CH<sub>4</sub> production pathway at depth, resulting from decomposition of complex organic matter, rather than fermentation of more simple C compounds, which would support acetoclastic methanogenesis (Fig 1). We report  
110 and discuss radiocarbon analyses of subsurface DOC, CH<sub>4</sub>, and CO<sub>2</sub> as well as peat biomolecular characterization using solid state <sup>13</sup>C-NMR spectroscopy in a tropical peatland.

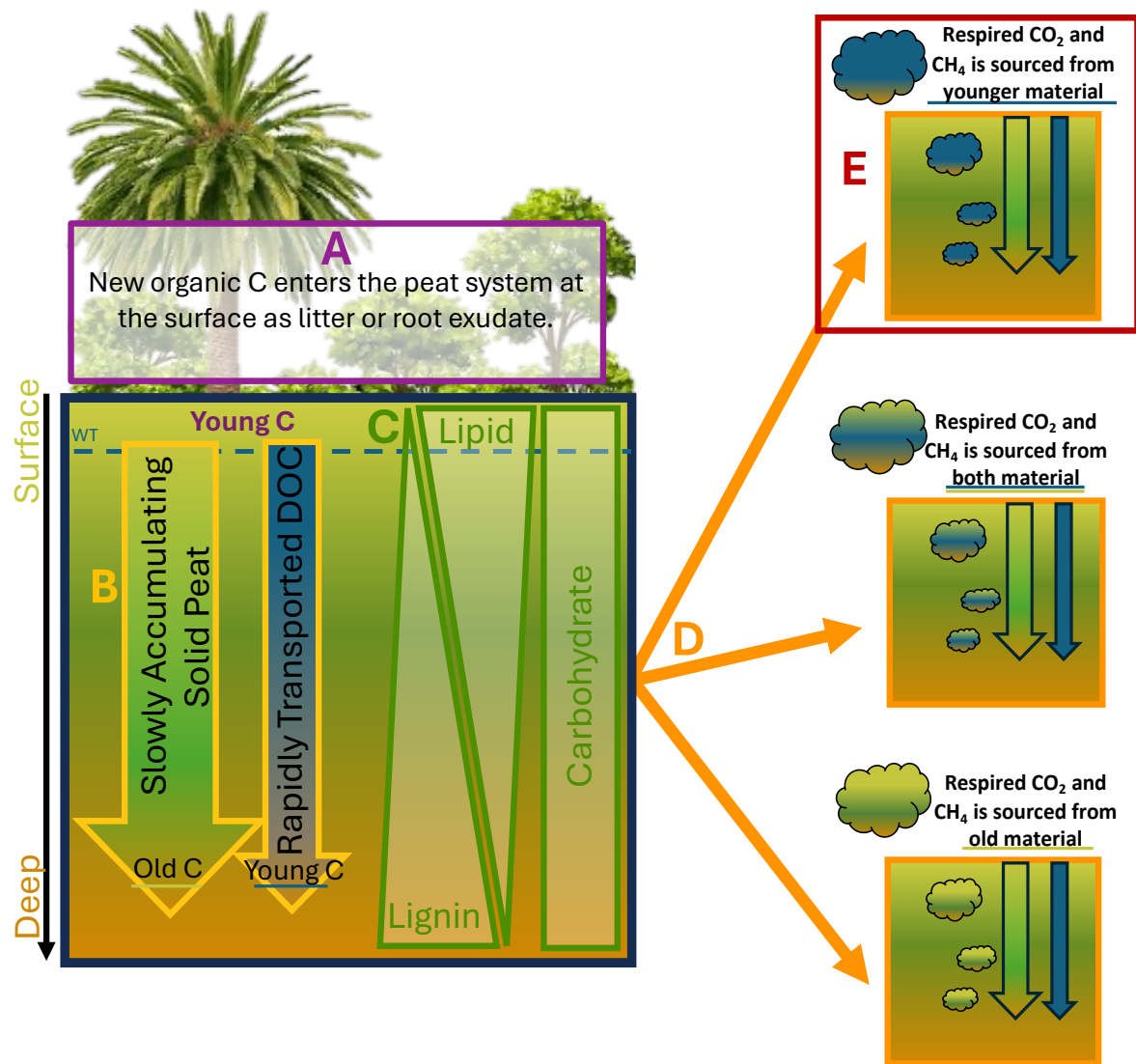


**Figure 1: Schematic illustrating our conceptual understanding of the tropical peat C cycle.** A) Surface vegetation acts as the primary source of new organic material entering the peat system. Key contributors include dead plant matter and root exudates, and lant species can influence the organic chemistry of C inputs to soils B) Slow accumulation of solid peat matter (green), versus the rapid fluxes of fresh, modern dissolved organic carbon (DOC) from the surface (blue) C) As bulk peat accumulates over time, decomposition alters the biochemical characteristics of solid peat down the soil profile, such as preferential preservation of lignin, a loss of lipids, and consistent carbohydrate content. D) Alternative scenarios are shown for gases produced within the peat soil exhibit C isotopic signatures that reflect the dominant source material, or a combination of both sources. Both organic inputs can contribute to gas production—either from a single source (top orange box and bottom orange box) or a mix of both (middle orange box). E) The results of this study indicate that the top scenario is most likely for these sites, with younger DOC fueling belowground respiration and methanogenesis, as illustrated in the red box.

## 2 Methods

### 2.1 Field Site Description

115           The Bocas del Toro Province on the Caribbean coast of Panama is home to San San Pond Sak, an internationally  
recognized Ramsar site (#611), which highlights the global significance of this wetland. This site includes the 80 km<sup>2</sup>  
Changuinola peat deposit, an ombrotrophic domed peatland located southeast of the Changuinola River (Fig. 2). Located 10  
km east from the peatland is the town of Bocas del Toro, Isla Colon, where the average annual rainfall and temperature are  
4000 mm and 30°C respectively (Isla Colon, STRI Environmental Monitoring Station). There is continuous rainfall throughout  
120 the year with no pronounced dry season, although there are two distinct periods of lower rainfall (February–April and  
September–October). The water table was consistently at the surface of the peatland throughout the sampling period, but has  
been reported to fluctuate from 20cm above to 40cm below the peat surface during high or low rainfall (Hoyos-Santillan,  
2014). Mean peat temperature 10 cm below the surface is 25 °C and shows little intra-annual variation (Wright et al., 2011).  
The oldest deposits in the peatland are in the centre of the dome, are estimated to have been formed 4000–4500 years ago, and  
125 are roughly 8 m deep (Phillips et al., 1997).

          The Changuinola peat deposit developed from *Raphia taedigera* palm swamp, unlike southeast Asia coastal peatlands  
that begin as sediment trapping mangrove stands (Anderson and Muller, 1975; Phillips et al., 1997). The vegetation  
communities that formed the Changuinola peat deposits have shifted spatially over time, reflecting variations in environmental  
conditions, and resulting in spatial heterogeneities in C inputs across the peatland (Cohen et al., 1989; Phillips and Bustin,  
130 1996). At present, there are seven distinct phasic plant communities that form concentric rings within the peat dome. From the  
periphery and moving to the interior they are as follows: (i) *Rhizophora mangle* mangrove swamp, (ii) mixed back mangrove  
swamp, (iii) *Raphia taedigera* palm swamp, (iv) mixed forest swamp, (v) stunted *Camposperma panamensis* forest swamp,  
(vi) sawgrass/stunted forest swamp and (vii) *Myrica-Cyrilla* bog-plain (Phillips et al., 1997). Previous work showed that  
nutrient content in the peat was generally higher near the edge (1200 µg-phosphorus (P)g<sup>-1</sup>, 27mg-nitrogen (N)g<sup>-1</sup>) and lower  
135 in the interior of the peatland (377 µg-Pg<sup>-1</sup>, 22mg-Ng<sup>-1</sup>) (Sjögersten et al., 2011; Troxler, 2007; Troxler et al., 2012).

140 For this study we selected sites in three of the representative plant communities, with dominant vegetation and nutrient patterns described previously. These include Outer (*Raphia taedigera* palm swamp), Intermediate (mixed forest swamp), and Inner (stunted *Camposperma panamensis* forest swamp) peatland sites (Fig. 2). Previous studies conducted within the Changuinola deposit have reported differences in peat properties, root exudate characteristics, and *ex situ* experimental response in lab studies tied to vegetation community (Girkin et al., 2018b, 2019; Sjögersten et al., 2011; Upton et al., 2018; Wright et al., 2013). Previously reported surface (<30 cm) CO<sub>2</sub> flux rates for the outer and inner sites used here varied from 320-500 mg CO<sub>2</sub> m<sup>-2</sup> hr<sup>-1</sup> with no significant variation between sites (Wright et al., 2011), and subsurface peat (below 30 cm) appeared to have similar carbohydrate to aromatic C ratios at the surface (Upton et al., 2018).

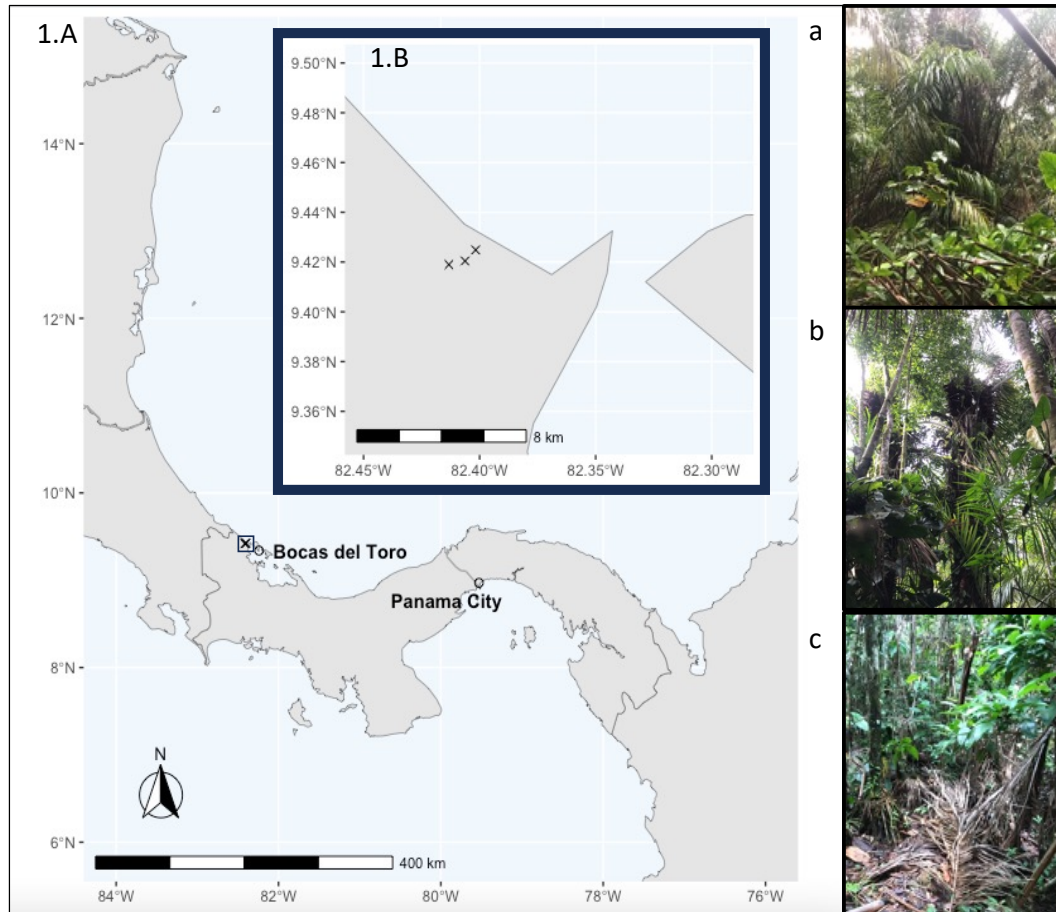


**Figure 2: Map of sites included in this study from the Changuinola peat deposit. A.** Location of study site identified by square in relation to the city of Bocas Del Toro and Panama City. **B.** Inset showing the location of the sites along the transect. The sites follow a vegetation gradient with a) the outer site closest to the channel *Raphia taedigera* palm swamp b) the intermediate site mixed forest swamp and c) the inner site closest to the centre of the peatland composed of stunted *Camposperma panamensis* forest swamp. The nutrient gradient decreases from outer site to inner site.

## 2.2 Sample Collection

145 Bulk peat, pore water samples, and greenhouse gases (CO<sub>2</sub> and CH<sub>4</sub>) were collected in October of 2019. We sampled from 30 cm to basal depths that were identified by a marine clay boundary at the base of the peat, and did not sample surface samples (0–30 cm) that might have stronger surface vegetation influence on peat chemistry compared to deeper layers that are further along in the decomposition process (Barreto and Lindo, 2020). This study aimed to compare bulk peat and pore water components of deep peat with gas produced at the same depth, and for that reason only those deeper samples were collected.

150 Peat cores were collected using a 5.2 cm diameter and 51 cm long peat sampler (Eijkelkamp, Product code 04.09). Bulk peat, pore water samples, and greenhouse gases (CO<sub>2</sub> and CH<sub>4</sub>) were collected in October of 2019 from depths of 30 ± 5 and 60 ± 5 cm, as well as 100 ± 5, 200 ± 5, 300 ± 5, and 400 ± 5 cm depending on total peat depth at each site. Porewater was collected using a peristaltic pump with Teflon tubing from 1.25 cm diameter PVC pipe piezometers to measure DOC from the same depths as the peat collection. Porewater was filtered with 45 um particle retention using plastic syringes fitted with stopcocks

155 and filters and deposited into 50 ml falcon tubes for transport. Following collection, peat cores were subsampled to coordinate with gas well depths and sealed in plastic bags to avoid oxidation during transport to the Smithsonian Tropical Research Institute soils lab in Panama City, Panama.

Diffusion gas wells were deployed at the intermediate and outer site at the same depths as pore water and peat collection to ensure robust comparison between the two source materials (bulk peat and DOC) and respiration products. There

160 was insufficient time to include the inner site in gas collection at time of sampling. These diffusion wells consisted of PVC pipe with mesh coverings positioned within the peat to allow water to be sampled from the desired depth without contamination of bulk peat or water pulled from other depths. Water was taken from the desired depth using a peristaltic pump and cycled into a 1L glass container. The headspace within the glass container was allowed to equilibrate over several hours while the water was pumped through the container at a rate of 1.5–1.8 L/min. Air samples from the equilibrated headspace were taken

165 using a syringe fitted with a stopcock and needle and deposited into evacuated 125 ml serum bottles fitted with heavy butyl rubber septa.

## 2.3 Elemental and Isotopic Analyses

Elemental composition of solid homogenized airdried peat was analysed using an elemental analyser 205 (CHNOS) coupled to an IsoPrime 100 isotope ratio mass spectrometer at the Center for Stable Isotope Biogeochemistry (CSIB) 206 at

170 the University of California, Berkeley. This analysis produced measurements for percent C and N content, <sup>13</sup>C, and <sup>15</sup>N. The ash content of bulk peat was determined by ignition of aliquots (~1.0 g) at 460°C for 5 hr.

Sample preparation and analysis for Δ<sup>14</sup>C was completed at the Center for Accelerator Mass Spectrometry (CAMS) at Lawrence Livermore National Laboratory. To ensure that peat samples were handled appropriately for both biogeochemistry and chronology, following homogenization with a ball and mill grinder we measured two subsamples; one that underwent

175 acid-base-acid (ABA) pre-treatment to remove possible interfering carbonates and modern C derived humic acids, and a second

with no pre-treatment (Norris et al., 2020). Samples were immersed in 1N hydrochloric acid (HCl) to remove carbohydrates. Humic acids were then removed from the sample with 0.25M sodium hydroxide (NaOH) and treated with a 1N HCL immersion before they were rinsed with deionized water until neutral. The pre-treated samples were then placed on a heating block until dried. The two sets of peat samples had identical  $\Delta^{14}\text{C}$  results and the no pre-treatment values were used in this study (Table 180 A1). The porewater DOC samples were acidified with 1N HCl at 70 °C to remove dissolved inorganic C and freeze dried. Both sets of peat samples and the residual DOC were loaded into quartz tubes with excess CuO and combusted at 900°C to ensure complete combustion to CO<sub>2</sub>.

Gas samples for CH<sub>4</sub> and CO<sub>2</sub> were extracted following the protocol outlined by McNicol et al (2020). For <sup>14</sup>CO<sub>2</sub> samples, a series of cryogenic traps were used to purify and isolate the CO<sub>2</sub>. For <sup>14</sup>CH<sub>4</sub> samples, the mixed composition field 185 samples were cryogenically purified to remove water and CO<sub>2</sub>, and the remaining CH<sub>4</sub> was converted to CO<sub>2</sub> by combustion (Petrenko et al., 2008). Resulting CO<sub>2</sub> from samples was split to measure both a  $\delta^{13}\text{C}$  and  $\Delta^{14}\text{C}$ . Extracted CO<sub>2</sub> and CH<sub>4</sub> were analysed for  $\Delta^{14}\text{C}$  and  $\delta^{13}\text{C}$  when possible, but some sample masses were too small for both analyses (minimum 20 ug C needed for  $\Delta^{14}\text{C}$  analysis and for the purpose of this study, we prioritized measurements for  $\Delta^{14}\text{C}$ ). The  $\delta^{13}\text{C}$  values were analysed at the Stable Isotope Geosciences Facility at Texas 210 A&M University on a Thermo Scientific MAT 253 Dual Inlet 190 Stable Isotope Ratio Mass Spectrometer. To obtain a  $\Delta^{14}\text{C}$  measurement, the CO<sub>2</sub> was reduced to graphite onto Fe powder in the presence of H<sub>2</sub> (Vogel et al., 1984) and analysed on the HVEC 10 MV Model FN Tandem Van de Graaff Accelerator or the NEC 1 MV Pelletron Tandem Accelerator at CAMS (Broek et al., 2021).  $\Delta^{14}\text{C}$  values are reported as  $\Delta^{14}\text{C}$  (‰) corrected to the year of measurement (2019) and for mass-dependent fractionation using  $\delta^{13}\text{C}$  values, and age is reported in years before present (yBP) within two standard deviations using the Libby half-life of 5568 years following the conventions outlined by 195 Stuiver and Polach, 1977. Age-depth models were generated for each site in R v.4.2.2 (The R Foundation for Statistical Computing, 2022) using the “rbacon” package v2.3.9.1. BACON (Bayesian accumulation), is based on Bayesian theory, and simulates the sediment deposition process while accounting for both variable deposition rates and spatial autocorrelation of deposition from one layer to another within the core. Long-term peat accumulation rates were estimated by fitting linear regressions to age-depth model outputs. The calibrated ages showed timing of peat development and accumulation between 200 the three sites, and the conventional radiocarbon values were used to compare and identify the sources of material used to generate CO<sub>2</sub> and CH<sub>4</sub> at depth.

Differences in stable isotopic ( $\delta^{13}\text{C}$ ) composition between  $\delta^{13}\text{CO}_2$  and  $\delta^{13}\text{CH}_4$  can identify the dominant pathway that produces methane, because hydrogenotrophic methanogenesis fractionate against heavy C isotopes more than acetoclastic methanogenesis (Wilson et al., 2016). Based on the measured stable carbon isotope signatures of CH<sub>4</sub> ( $\delta^{13}\text{C-CH}_4$ ) and CO<sub>2</sub> ( $\delta^{13}\text{C-CO}_2$ ) in dissolved gas in peat pore water, we calculated the apparent carbon isotope fractionation ( $\alpha_{\text{app}}$ ) for this 205 methanogenic process according to formula:  $\alpha = (\delta^{13}\text{CO}_2 + 1000) / (\delta^{13}\text{CH}_4 + 1000)$ . Values of  $\alpha_{\text{app}} = [(\delta^{13}\text{CO}_2 + 1000) / (\delta^{13}\text{CH}_4 + 1000)]$  that are greater than 1.065 are characteristic of environments dominated by hydrogenotrophic methanogenesis, while values lower than 1.055 are characteristic of environments dominated by acetoclastic methanogenesis (Zhang et al., 2019).

## 210 2.4 <sup>13</sup>C-NMR Spectroscopy and Mixing Model

Solid State <sup>13</sup>C NMR spectra of untreated peat samples were obtained at the Pacific Northwest National Laboratory in Washington state at the Environmental Molecular Science Laboratory facility using cross-polarization under magic angle spinning conditions (CP/MAS) with a Varian Direct Drive NMR spectrometer equipped with a Varian 4-mm probe. These bulk peat samples were free of charcoal. Approximately 30 mg of peat were packed in 4 mm zirconia rotors sealed with Kel-  
215 F caps. The CP spectra were acquired after 14k scans with a MAS rate of 14 kHz resulting in no interference from sidebands as they were outside the range of the spectrum, and a ramp-CP contact time on proton of 1 ms and a 1 or 2 s recycle delay depending on the sample with 62.5 kHz tppm proton decoupling (Aliev, 2020). The one-dimensional <sup>1</sup>H NMR spectra of all samples were processed and analysed relative to the external standard adamantane. All spectra were corrected against a KBr background, and signals arising from C in the NMR probe and rotor were accounted for by subtracting the spectra of an empty  
220 rotor from the sample. Spectra were digitally processed with exponential apodization (100 Hz line broadening with the first point set to 0.50), phase correction, and baseline correction using a Bernstein polynomial fit with Mnova software (v. 14.3.3; Mestrelab Research). Peak areas were integrated within seven chemical shift regions for input to the molecular mixing model corresponding to: alkyl C (0–45 ppm), N-alkyl/methoxyl C (45–60 ppm), O-alkyl C (60–95 ppm), di-O-alkyl (95–110), aromatic C (110–145 ppm), phenolic C (145–165 ppm), and carboxyl C (165–215 ppm).

225 We used a mixing model which incorporates six components to describe the molecular composition of samples based on <sup>13</sup>C NMR outputs (Baldock et al., 2004). This peatland soil has no visual evidence of char, so that component was removed from the model. The five remaining components (carbohydrate, protein, lipid, lignin, and carbonyl) have each been assigned a discrete percent of different regions of the <sup>13</sup>C NMR signal intensity based on knowledge of molar elemental contents and C content of terrestrial soil ecosystems. The measured C:N ratio of each sample was used to constrain the protein concentration  
230 of each <sup>13</sup>C NMR spectrum in the molecular mixing model. The optimisation process of the molecular mixing model compares fits for all five biomolecules to models eliminating one, two, and three components; in all cases the model fit was best when all five components were included in the model (sum of squares of deviation < 6%). The mixing model outputs are available in Table A2.

## 2.6 Statistics

235 We assessed our data at two scales: 1) among-site comparisons of the three sites, considering overall differences in peat characteristics and isotopic signatures and 2) peatland-wide patterns in soil profile characteristics and relationships among peat chemistry and isotopic signatures. Relationships between peat physical properties (C and N concentrations, C:N, <sup>13</sup>C, <sup>15</sup>N, and radiocarbon) and the five biomolecules identified with the molecular mixing model were assessed using Pearson correlation analysis. We also conducted separate analyses of the <sup>13</sup>C-NMR data using raw data for spectral regions. The three  
240 sites were pooled to get peatland scale relationships between the peat physical properties and the five biomolecules versus depth. Due to the limited size of this dataset, the spearman method was used to measure covariance and the coefficients are

reported in the full correlation matrix results, including  $r^2$  values and significance, in supplementary materials (Fig. A3 & A4). We assessed differences among the three sites using Principal Component Analysis (PCA) based on all factors included in the correlation matrices (all peat physical properties, chemistry, and isotopes for each site). Significant trends in biomolecule abundance across depth were identified by linear regression. To identify differences between mean radiocarbon values of the sources and respiration products we utilized two-sample t-tests. Bulk peat and gas products were determined by Welch two-sample t-test to account for lack of homogeneity of variance, and differences between mean radiocarbon values of DOC and gas products were assessed by student two sample t-test. All relationships explored were considered significant at the 0.1 alpha level. Statistical analyses were conducted in R v.4.2.2 (The R Foundation for Statistical Computing, 2022). Reported means in the text are shown with standard errors in parentheses.

### 3 Results

#### 3.1 Isotopic composition of source material and respiration products

Across all sites and depths, dissolved  $\text{CH}_4$  and  $\text{CO}_2$  were relatively modern,  $^{14}\text{C}$ -enriched relative to peat, and had similar  $\Delta^{14}\text{C}$  values to DOC, indicating the use of DOC as a preferential substrate over solid peat for microbial respiration (Fig 3). Overall, the respiration products had statistically similar values to the DOC ( $t(23)=0.534$   $p=0.60$ ) compared to the bulk peat ( $t(16)=|8.67|$ ,  $p=<0.05$ ) (Table S3). The radiocarbon values for the bulk peat are consistent with constant accumulation over time. The calibrated basal ages for outer, intermediate, and inner sites were  $1215 \pm 35$ ,  $1060 \pm 30$ , and  $1750 \pm 35$  yrBP respectively.

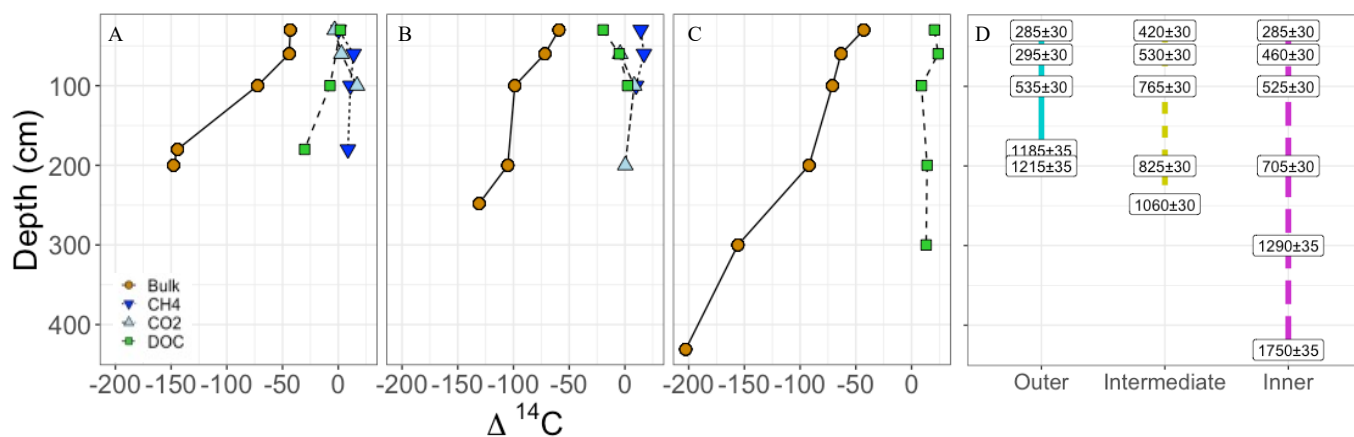


**Figure 3. Isotopic composition of respiration products and substrates.** Bulk peat, DOC, and respiration products ( $\text{CH}_4$  = methane,  $\text{CO}_2$  = carbon dioxide) plotted by depth across all three sites; **A**) Outer, **B**) Intermediate and **C**) Inner. Brown circles and solid lines represent bulk peat and green squares with dashed lines represent DOC; these are the two measured sources available for gas production. The gas products are denoted by inverted dark blue triangles and dotted lines for methane, and the light blue triangles and dashed lines for dissolved carbon dioxide. Note the age difference between solid peat and all DOC and gas values; this offset indicates that gas production is driven by modern DOC throughout the peat profile. **D**. Calibrated ages for all bulk peat measured in yBP within two standard deviations for the outer, intermediate, and inner sites denoted by solid blue, dashed yellow, and dashed pink respectively.

### 3.2 Peat Properties and Chemistry

260 The percent OC across the sites was consistently 40–55% down to basal depths, which had lower OC contents and higher ash content, reflecting the influence of underlying mineral sediments (Fig. 4). The negative correlation between both OC and N concentrations with depth was not significant, however the negative correlations between ash content and depth ( $r(16) = -0.62, p \leq 0.1$ ) and age and depth ( $r(16) = -0.93, p \leq 0.1$ , Fig. 4) were strongly significant (Fig. A3). Bulk peat stable isotopes,  $\delta^{13}\text{C}$  and  $\delta^{15}\text{N}$ , showed no strong relationship with depth or site. Linear slopes across the age-depth profiles suggested  
265 consistent peat accumulation rates across the peatland over time (Fig. 4f). Estimates of long-term peat accumulation rates were calculated using the calibrated ages, and were  $0.192 \text{ cm yr}^{-1}$ ,  $0.473 \text{ cm yr}^{-1}$ , and  $0.275 \text{ cm yr}^{-1}$  for the outer, intermediate, and inner sites respectively.

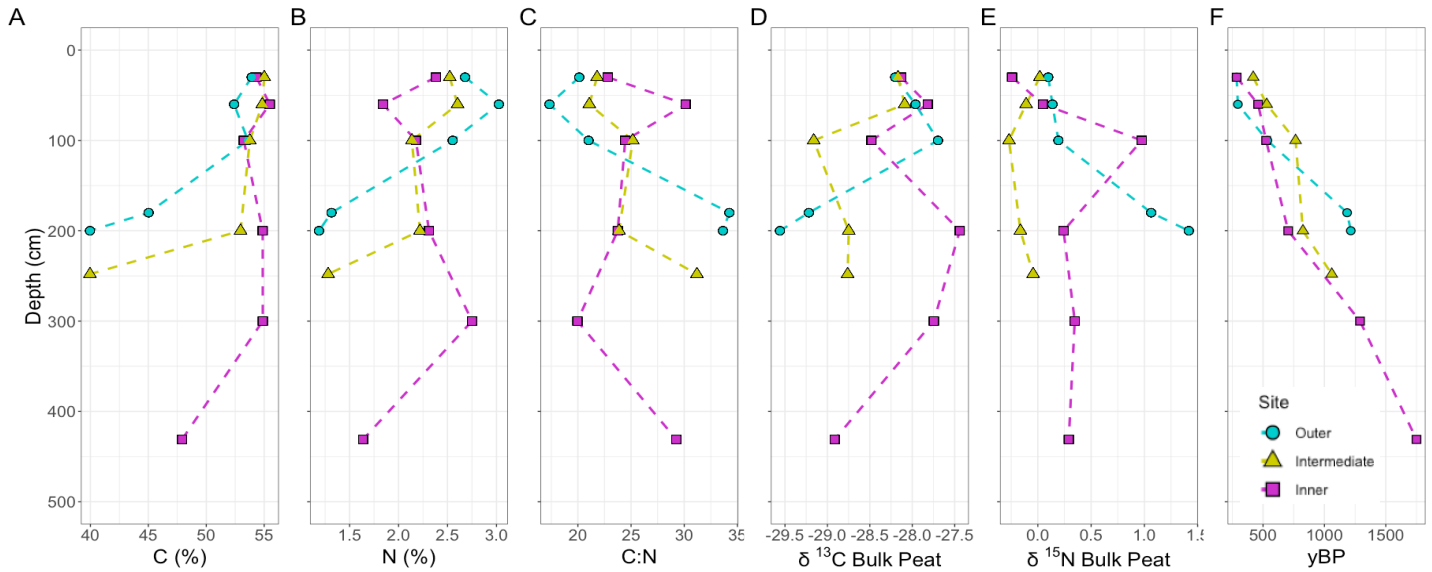


**Figure 4. Bulk Peat Properties and Characteristics.** Depth profiles for A. percent carbon, B. percent nitrogen, C. the ratio of carbon to nitrogen, D. stable carbon isotope, E. stable nitrogen isotope, and E. calibrated age for layers measured for the three sites. Sites are indicated by colour and shape with blue circles indicating the outer site, yellow triangles the intermediate site, and pink squares the inner site.

2%  $\pm$  2 carbonyl-C respectively (Fig 6. A&C). Overall, the organic chemistry of peat was very similar across the sites explored here, and the main patterns that emerged were trends with depth.

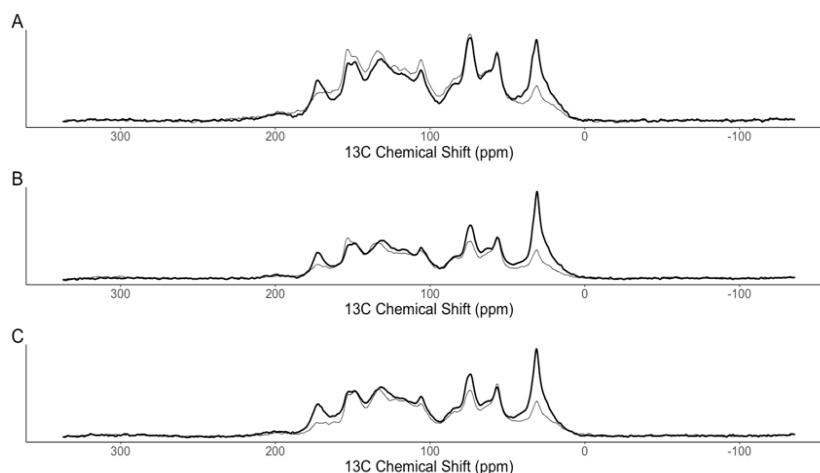
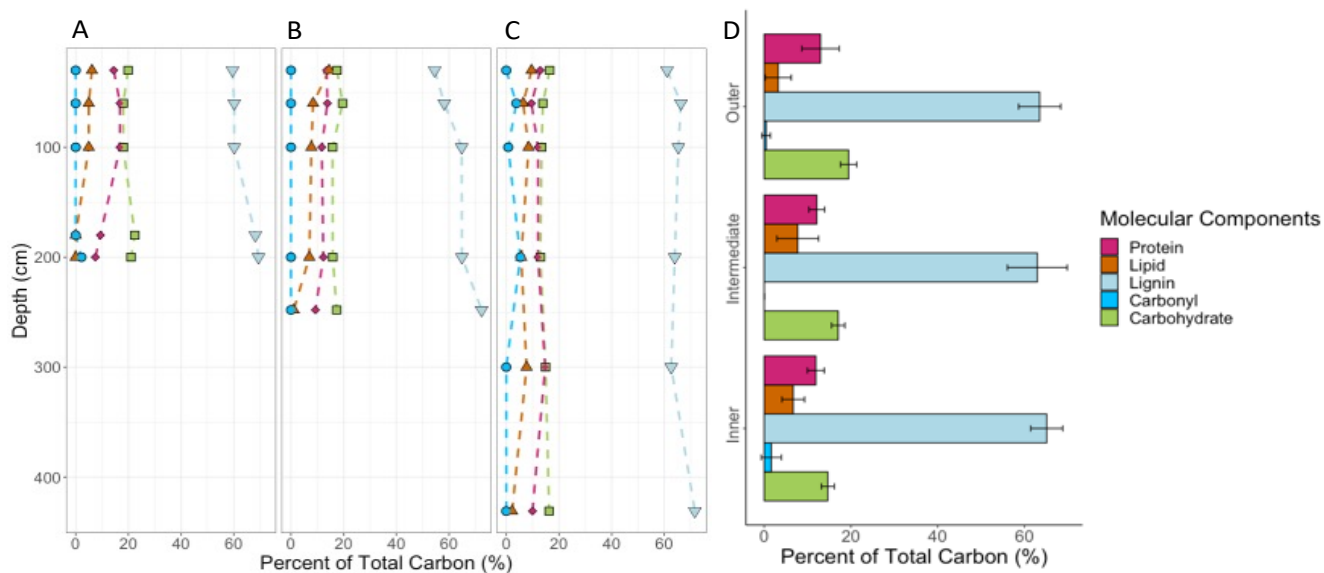


**Figure 5. Example  $^{13}\text{C}$  NMR spectra.** Bulk peat layers sampled from the A. outer, B. intermediate, and C. inner sites showing differences between the shallow (bold) and basal (thin) depths with stacked spectra; the complete spectra dataset can be found in additional data located in supplemental material. Spectra were digitally processed with Mnova software (v. 14.3.3; Mestrelab Research) with exponential apodization (100 Hz line broadening with the first point set to 0.50), phase correction, and baseline correction using a Bernstein polynomial fit.



280 We used PCA to explore differences in peat properties among the three sites. The scores and loadings of the first and second principal components accounted for the majority of variance (74%) with the first principal component accounting for 54.93% (Fig 7). Separation along the first principal component axis showed stratigraphic effects related to depth and peat accumulation over time, with strong separation between the 30 and 60 cm layers versus the underlying peat. The clustering of the 30 and 60 cm peat layers was primarily driven by OC and N concentration, age, ash content, and lipid, alkyl-C, and protein contributions to soil OC (Fig 7, Table A2). By contrast, the second principal component was mainly driven by site differences, with the inner site being relatively more distinct than the outer and intermediate sites while still showing some overlap (Fig 7).  
 285 This separation appeared to be tied to the small amount of carbonyl present at this site (Fig 7, Table A2, Table A4).

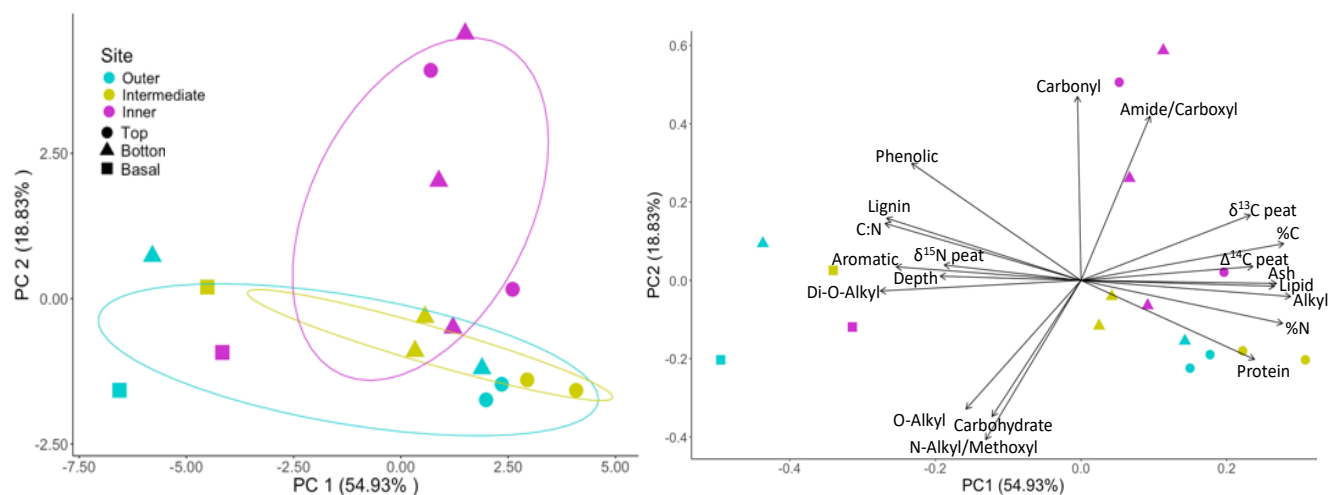


**Figure 7. Scores and loadings from the PCA** for all peat properties and chemistry and depth for the outer (blue), intermediate (yellow), and inner (pink) sites. Depths have been indicated by shape with the top (30-60 cm) as circles, the bottom (>1 m) as triangles, and the three basal depths as squares (basal depths; Outer 200 cm, Intermediate 248 cm, and Inner 431 cm). Combined PC1 and PC2 account for 74% of variance.

### 290 3.3 Using $\delta^{13}\text{C}$ to identify $\text{CH}_4$ Production Pathway

The  $\alpha_{\text{app}}$  values overlap between the outer and intermediate sites and averaged 1.078 (+/- 0.003) (Fig. 8). These data demonstrate no shift in  $\alpha_{\text{app}}$  with depth throughout the peat profile. The  $\alpha_{\text{app}}$  is consistent with hydrogenotrophic methanogenesis being the dominant production pathway across all depths measured at the outer and intermediate sites.

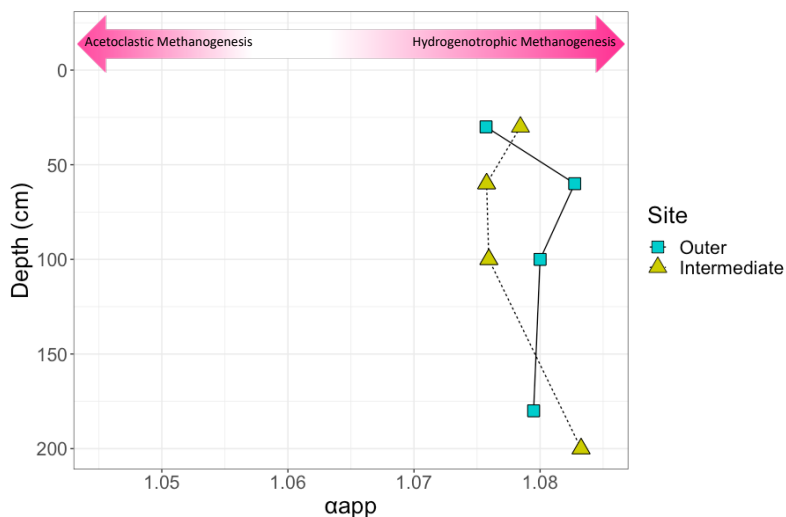


**Figure 8. Differences in stable C isotopic composition between DIC and  $\text{CH}_4$ .** Calculated estimates of apparent fractionation factor ( $\alpha_{\text{app}}$ ) across depth for gas collected from the outer (blue squares) and intermediate (green triangles) sites. The samples from the inner site did not have sufficient amounts of C for this analysis. Note the x-axis shows little variation in  $\alpha_{\text{app}}$  between sites and soil layers; values of  $\alpha_{\text{app}}$  higher than 1.065 is usually characteristic of environments dominated by hydrogenotrophic methanogenesis, while a value lower than 1.055 is characteristic of an environment dominated by acetoclastic methanogenesis (Corbett et al., 2013).

## 4. Discussion

### 295 4.1 Source

The Changuinola peat deposit is important as an internationally protected wetland and is an example of a pristine undisturbed functioning tropical peatland. This is supported by the age-depth profiles that showed continuous undisturbed peat accumulation over time, and similarities in OC and N concentrations and C:N ratios to other ombrotrophic peat domes across the tropics (Beilman et al., 2019; Dargie et al., 2017; Lahteenoja et al., 2012; Omar et al., 2022). This paper contributes a novel  
300 characterization of the organic components contributing to surface  $\text{CO}_2$  and  $\text{CH}_4$  fluxes (bulk peat, respiration products, peat chemical composition) to identify the dominant source of OC for a tropical peatland. Across all sites and depths, DOC exhibited enriched radiocarbon signatures compared to the bulk peat, indicating it is largely derived from recent photosynthate. This suggests that while the DOC originates from newer organic material, the solid peat becomes progressively older with depth, confirming that the peat found in deeper layers is indeed older. Most importantly, we demonstrate that while both of these

305 sources are available for utilization, the respiration products closely resemble, if not completely match, the DOC, indicating that DOC is currently the source of CO<sub>2</sub> and CH<sub>4</sub> in this peatland.

Similar behaviour has been reported in other tropical peatlands that preferentially use modern DOC as the source for microbial respiration ( Hoyt et al., 2020), while one site in Borneo reported respiration products from mixed sources (Hoyt, 2014). These contrasting results suggest either the Borneo peatland site is an exception to this behaviour or there is need to  
310 explore more tropical peatland sites to characterize source selection behaviour in the tropics. Our findings indicate that surface-derived DOC significantly influences gas production deep within the soil profile, potentially linked to the high lignin content typical of wood-dominated peatlands. At our sites, contrasting surface vegetation types—*Raphia taedigera* and mixed  
315 Even at greater depths, the influence of surface vegetation remains significant, underscoring the importance of surface-derived DOC for carbon dynamics in these ecosystems. Tropical peatlands with higher abundances of sedge or shrub species may exhibit different source selection preferences based on variations in DOC, root exudates, and peat composition (Girkin et al., 2018a; Waldron et al., 2019).

#### 4.2 Peat Chemistry and Stabilization

320 The dominant biomolecule making up this peat OC was lignin, which generally represented >60% of the OC in our samples. Despite the lack of a depth difference in the aromaticity index, we saw an accumulation of lignin with depth, indicating preferential preservation of this biomolecule and microbial discrimination against its decomposition through time. This selective preservation of lignin has been reported for this wetland (Hoyos-Santillan et al., 2016) and other tropical peatlands (Gandois et al., 2014) previously, and supports a paradigm of selective preservation of aromatic compounds under  
325 anaerobic conditions. Coarse woody material from fallen trees, branches, and dead roots contribute a large yet relatively sporadic portion of OC inputs to tropical peat, in addition to the more constant inputs from leaf litter and fine root turnover (Hodgkins et al., 2018), and our data together with the previous studies indicate that this large-scale tree mortality and branch shedding is crucial for peat OC accumulation. The waterlogged conditions in tropical peatlands can particularly reduce the decomposition of lignin by inhibiting ligninolytic microbes (Hoyos-Santillan et al., 2015; Thormann, 2006). There was little  
330 change in the carbohydrate portion of peat OC with depth, even though carbohydrates typically represent the most labile compounds in plant tissues for decomposition (Bader et al., 2018). This lack of change in carbohydrate abundance with depth below 30 cm may indicate consistent preservation of this molecule after any initial decomposition in the top 30 cm, and contrasts with the preferential preservation of lignin. Interestingly, we see a significant decline in lipids with depth, even though other tropical and temperate forest studies have indicated preferential preservation of lipids in upland soils (Cusack et al., 2018; Jastrow et al., 2007; Wiesenberg et al., 2010). Our data suggest that under anaerobic conditions, lipids are  
335 decomposed more than other compounds, and/or microbial biomass production of lipids declines, or changes in carbon inputs over time. Taken together, our data support different decomposition rates and preservation processes of individual biomarkers

that contribute to the accumulation of OC within tropical peatlands. Specifically, there is evidence of varying rates of biomarker degradation related to the composition of the organic matter in these sites, suggesting that certain compounds are more resistant to decomposition (Girkin et al., 2018a). Meanwhile, specific environmental conditions and microbial communities can also influence the preservation of these biomarkers, further supporting our findings that the interplay between biological origin and decomposition processes is critical for understanding OC dynamics in tropical peatlands (Hoyos-Santillan et al., 2016). Together, these studies reinforce the complexity of OC dynamics and the significance of individual biomarkers in shaping C storage within these ecosystems.

Our outer site is closest to the edge of the peatland in an area in the peatland that is dominated by *Raphia taedigera* palm swamp and with relatively high nutrient availability, while the intermediate site dominated by mixed forest swamp species, and the inner site closest to the centre of the peatland dominated by stunted *Camposperma panamensis* forest and has relatively low nutrient availability (Phillips and Bustin, 1996; Sjögersten et al., 2011; Troxler, 2007). Despite these documented differences, we found strong similarity across sites in peat characteristics as well as the radiocarbon content of porewater DOC, CO<sub>2</sub>, and CH<sub>4</sub>. Our results demonstrate that the peat at or below 2 m is relatively carbohydrate- and lignin-rich and potentially less decomposed than expected, making these soils vulnerable to rapid decomposition if exposed to aerobic conditions.

Based on the  $\Delta^{14}\text{C}$  and age of peat collected across these sites, the dome shape of the peatland has built up with older layers closer to the surface at the margins (Fig 9). This shape and accumulation pattern has been described and modelled across other tropical peat domes that have the similar ombrotrophic characteristics as Changuinola (Cobb et al., 2017, 2024). Our results suggest age was not a driver of peat chemical characteristics or properties that describe decomposability, and that older peat that accumulated over 1000 years ago is closer to the surface at the margins and would be the first layers to experience aerobic conditions with changes in water table draw down or disturbance (Dommain et al., 2011).

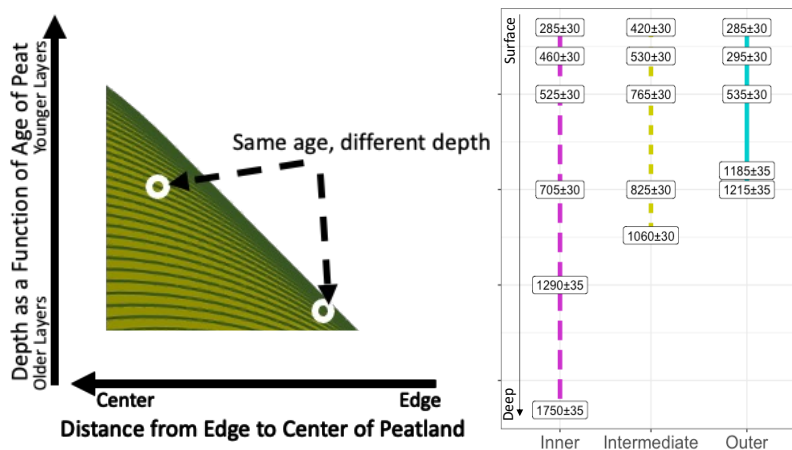


**Figure 9: Schematic of peatland shape and layer accumulation pattern based on peat layer age and depth from surface.** This concept was presented in model data from Cobb et al., 2017 and has been modified to create this schematic that is not to scale. Peat layers accumulate over time with the youngest layers at the surface and oldest layers at the base of the peat deposit. Based on this and ages collected from the sites within the Changuinola peat deposit, layers that correspond to the same age are located at different depths across the peat dome with older peat layers are closer to the surface at the margins.

## Using $\delta^{13}\text{C}$ to understand $\text{CH}_4$ Production

Peat organic matter quality not only influences decomposition rates but also affects the pathway of  $\text{CH}_4$  production (Holmes et al., 2015). When easily degradable inputs are decomposed, acetate is produced by fermentative bacteria, enhancing the role of acetoclastic methanogenesis (Mobilian and Craft, 2022). As labile material becomes depleted, the decomposition of more resistant compounds and the associated  $\text{CO}_2$  production promote a shift toward hydrogenotrophic methanogenesis (Conrad, 2020). The high observed  $\alpha_{\text{app}}$  ( $1.078 \pm 0.003$ ) within this study suggests that hydrogenotrophic methanogenesis is the primary  $\text{CH}_4$  production pathway, with no evidence of depth-related variation. These findings align with Holmes et al. (2015), who reviewed fractionation factors across global peatlands.

While we cannot map the exact progression from plant material to  $\text{CH}_4$ , hydrogenotrophic methanogenesis depends on  $\text{CO}_2$  availability for reduction to  $\text{CH}_4$ , with  $\text{CO}_2$  from initial decomposition steps likely serving as a key source (Gruca-Rokosz and Koszelnik, 2018; Kotsyurbenko et al., 2004). This cooperative microbial interaction, where primary degraders supply necessary precursors (in this case,  $\text{CO}_2$ ) for further metabolism, has been observed in soils and may regulate  $\text{CO}_2$  release within this peatland (Chen et al., 2023; Li et al., 2021). Further investigation into the methanogen community structure and stratigraphy is needed to better understand the factors affecting net  $\text{CH}_4$  flux from this wetland and to determine whether surface processes could alter  $\text{CH}_4$  production pathways in the upper (0–30 cm) peat layer.

Although both northern and tropical peatlands may exhibit hydrogenotrophic methanogenesis as the dominant pathway, the  $\delta^{13}\text{C}$ - $\text{CH}_4$  signature differs widely due to variations in precursor  $\delta^{13}\text{C}$ - $\text{CO}_2$ , influenced by temperature, microbial activity, organic matter composition, and decomposition processes (Holmes et al., 2015). In cold, highly anoxic northern peatlands,  $\delta^{13}\text{C}$ - $\text{CO}_2$  tends to be more depleted due to extensive carbon recycling in low temperatures and high water tables, which slows organic matter decomposition and allows for greater microbial processing that further depletes  $\delta^{13}\text{C}$  (Rinne et al., 2022). In contrast, the warmer, more readily decomposable organic material in tropical peatlands results in less depleted  $\delta^{13}\text{C}$ - $\text{CO}_2$  values (Holmes et al., 2015). While this study does not imply that tropical peatlands function differently from temperate peatlands, these findings suggest that research in higher-latitude peatlands offers a basis to explore OC cycling in tropical peatlands. However, additional validation is needed to confirm that they operate similarly.

## Future Implications

Tropical peatlands, such as the Changuinola peat deposit, represent critical carbon-rich ecosystems that play a substantial role in the global carbon cycle but face vulnerability under future climate scenarios. Our findings show that these peatlands currently rely heavily on surface-derived DOC to support deep peat respiration, produce  $\text{CH}_4$  primarily through hydrogenotrophic methanogenesis, and continue to accumulate lignin-rich, carbon-dense peat under anaerobic conditions. However, this carbon storage mechanism is sensitive to shifts in climate, hydrology, and vegetation. Changes in precipitation patterns and increased evapotranspiration associated with climate change could disrupt the connectivity between surface and

390 deep peat layers, altering DOC transport and potentially increasing the exposure of preserved peat to aerobic conditions. The  
predominance of lignin, resistant under anoxic conditions, raises questions about its vulnerability when exposed to oxygen. If  
peatlands dry out, the preserved OC could rapidly decompose, shifting the ecosystem from a sink to a potential carbon source,  
with significant greenhouse gas release (Kettridge et al., 2015; Ofiti et al., 2023).

395 Our study underscores the need for further research on the resilience of tropical peatlands under changing environmental  
conditions. Key areas for future work include examining how shifts in vegetation and surface inputs could influence OC  
dynamics and gas production. Variations in plant community composition and changes in nutrient status may affect DOC  
quality and quantity, potentially altering the balance between acetoclastic and hydrogenotrophic methanogenesis pathways.  
Additionally, further investigation into the microbial communities driving peat decomposition and CH<sub>4</sub> production could yield  
insights into how these processes may shift with changing environmental factors.

400 Comparative studies between high-latitude and tropical peatlands highlight the unique characteristics of tropical systems,  
which are subject to faster biomass production and decomposition rates in warmer climates. Unlike high-latitude peatlands,  
which accumulate OC slowly over millennia, tropical peatlands maintain a more dynamic OC balance. This difference suggests  
that tropical peatlands may be particularly vulnerable to rapid changes in hydrology and land use. Understanding how such  
factors interact to influence peat accumulation, organic matter preservation, and greenhouse gas flux is essential for assessing  
the stability of tropical peatlands in a warming world.

405 To fully realize the climate mitigation potential of tropical peatlands, future studies must address how these ecosystems  
respond to both gradual and abrupt environmental changes. The development of long-term conservation and restoration  
strategies will depend on our ability to anticipate the impacts of altered hydrology and vegetation composition on peatland OC  
storage. Continued research into these processes is vital for informing global climate policies and ensuring the preservation of  
these irreplaceable OC reservoirs.

410

Appendix A

415

Table A1: Radiocarbon results for both untreated (No Acid-Base-Acid) and treated (Acid-Base-Acid) sets of peat samples. Radiocarbon concentration is expressed as  $\Delta^{14}\text{C}$  within two standard deviations.

Site	Depth	$\Delta^{14}\text{C}$ (No ABA)	$\pm$	$\Delta^{14}\text{C}$ (ABA)	$\pm$
Outer	100	-72.4	3.1	-77.5	4.0
	180	-147.8	3.2	-157.6	3.6
	200	-144.3	3.2	-157.8	3.6
	30	-43.1	3.4	-54.9	4.1
	60	-44.0	3.4	-54.2	4.1
Intermediate	30	-59.2	3.4	-59.9	4.0
	60	-71.8	3.3	-70.2	4.0
	100	-98.8	3.3	-107.5	3.8
	200	-105.1	3.2	-110.8	3.8
	248	-130.8	3.2	-141.0	3.7
Inner	30	-42.9	3.3	-45.6	4.1
	60	-63.3	3.3	-68.5	4.0
	100	-71.0	3.2	-75.9	4.0
	200	-92.0	3.3	-93.6	3.9
	300	-155.8	3.2	-155.2	3.6
	431	-202.7	3.1	-203.1	3.4

420

425

Table A2: **Mixing model outputs for all depths sampled from the three sites.** Molecular component proportion of total C measured via  $^{13}\text{C}$ NMR described by the mixing model output as weighted percent (Wt%) developed by Baldock et al., 2004, %C measured from bulk peat combustion via elemental analyzer.

Site	Depth (cm)	Molecular Component	Wt%	%C
Inner	30	Carbohydrate	16.5	54.33
Inner	30	Protein	12.9	54.33
Inner	30	Lignin	61.0	54.33
Inner	30	Lipid	9.6	54.33
Inner	30	Carbonyl	0.0	54.33
Inner	60	Carbohydrate	13.9	55.49
Inner	60	Protein	9.6	55.49
Inner	60	Lignin	66.3	55.49
Inner	60	Lipid	6.4	55.49
Inner	60	Carbonyl	3.8	55.49
Inner	100	Carbohydrate	13.4	53.24
Inner	100	Protein	12.1	53.24
Inner	100	Lignin	65.3	53.24
Inner	100	Lipid	8.5	53.24
Inner	100	Carbonyl	0.7	53.24
Inner	200	Carbohydrate	13.0	54.87
Inner	200	Protein	12.1	54.87
Inner	200	Lignin	64.0	54.87
Inner	200	Lipid	5.7	54.87
Inner	200	Carbonyl	5.3	54.87
Inner	300	Carbohydrate	14.9	54.88
Inner	300	Protein	14.8	54.88
Inner	300	Lignin	62.6	54.88
Inner	300	Lipid	7.7	54.88

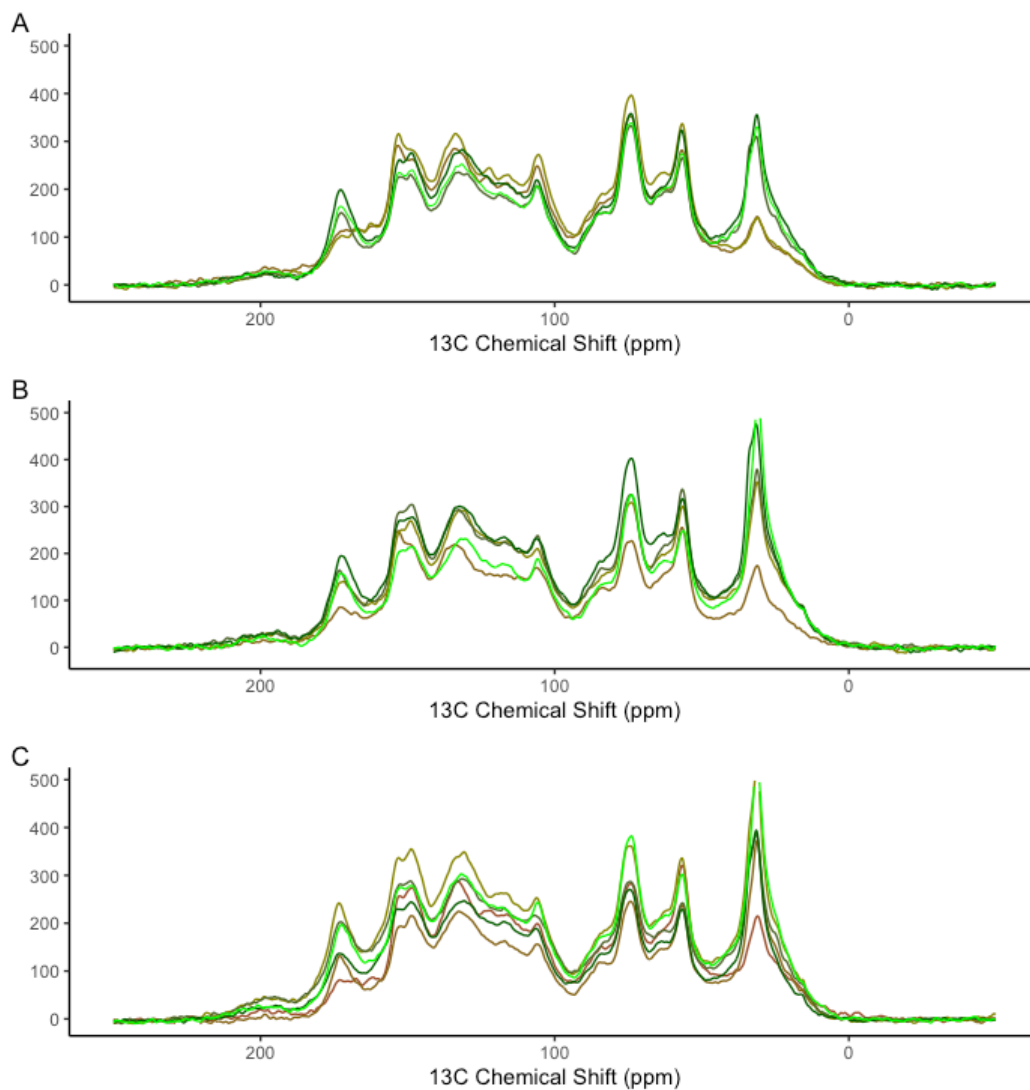
Inner	300	Carbonyl	0.0	54.88
Inner	431	Carbohydrate	16.3	47.91
Inner	431	Protein	9.9	47.91
Inner	431	Lignin	71.6	47.91
Inner	431	Lipid	2.2	47.91
Inner	431	Carbonyl	0.0	47.91
Intermediate	30	Carbohydrate	17.4	55.01
Intermediate	30	Protein	13.5	55.01
Intermediate	30	Lignin	54.5	55.01
Intermediate	30	Lipid	14.5	55.01
Intermediate	30	Carbonyl	0.0	55.01
Intermediate	60	Carbohydrate	19.6	54.84
Intermediate	60	Protein	13.8	54.84
Intermediate	60	Lignin	58.2	54.84
Intermediate	60	Lipid	8.4	54.84
Intermediate	60	Carbonyl	0.0	54.84
Intermediate	100	Carbohydrate	15.8	53.76
Intermediate	100	Protein	11.7	53.76
Intermediate	100	Lignin	64.8	53.76
Intermediate	100	Lipid	7.7	53.76
Intermediate	100	Carbonyl	0.0	53.76
Intermediate	200	Carbohydrate	15.9	52.96
Intermediate	200	Protein	12.3	52.96
Intermediate	200	Lignin	64.9	52.96
Intermediate	200	Lipid	7.0	52.96
Intermediate	200	Carbonyl	0.0	52.96
Intermediate	248	Carbohydrate	17.3	39.96

Intermediate	248	Protein	9.3	39.96
Intermediate	248	Lignin	72.4	39.96
Intermediate	248	Lipid	1.0	39.96
Intermediate	248	Carbonyl	0.0	39.96
Outer	30	Carbohydrate	19.9	53.92
Outer	30	Protein	14.4	53.92
Outer	30	Lignin	59.5	53.92
Outer	30	Lipid	6.2	53.92
Outer	30	Carbonyl	0.0	53.92
Outer	60	Carbohydrate	18.1	52.40
Outer	60	Protein	16.8	52.40
Outer	60	Lignin	60.2	52.40
Outer	60	Lipid	5.0	52.40
Outer	60	Carbonyl	0.0	52.40
Outer	100	Carbohydrate	18.1	53.60
Outer	100	Protein	16.8	53.60
Outer	100	Lignin	60.2	53.60
Outer	100	Lipid	5.0	53.60
Outer	100	Carbonyl	0.0	53.60
Outer	180	Carbohydrate	22.4	39.96
Outer	180	Protein	9.4	39.96
Outer	180	Lignin	68.2	39.96
Outer	180	Lipid	0.0	39.96
Outer	180	Carbonyl	0.0	39.96
Outer	200	Carbohydrate	21.0	45.03
Outer	200	Protein	7.5	45.03
Outer	200	Lignin	69.4	45.03

Outer	200	Lipid	0.0	45.03
Outer	200	Carbonyl	2.2	45.03

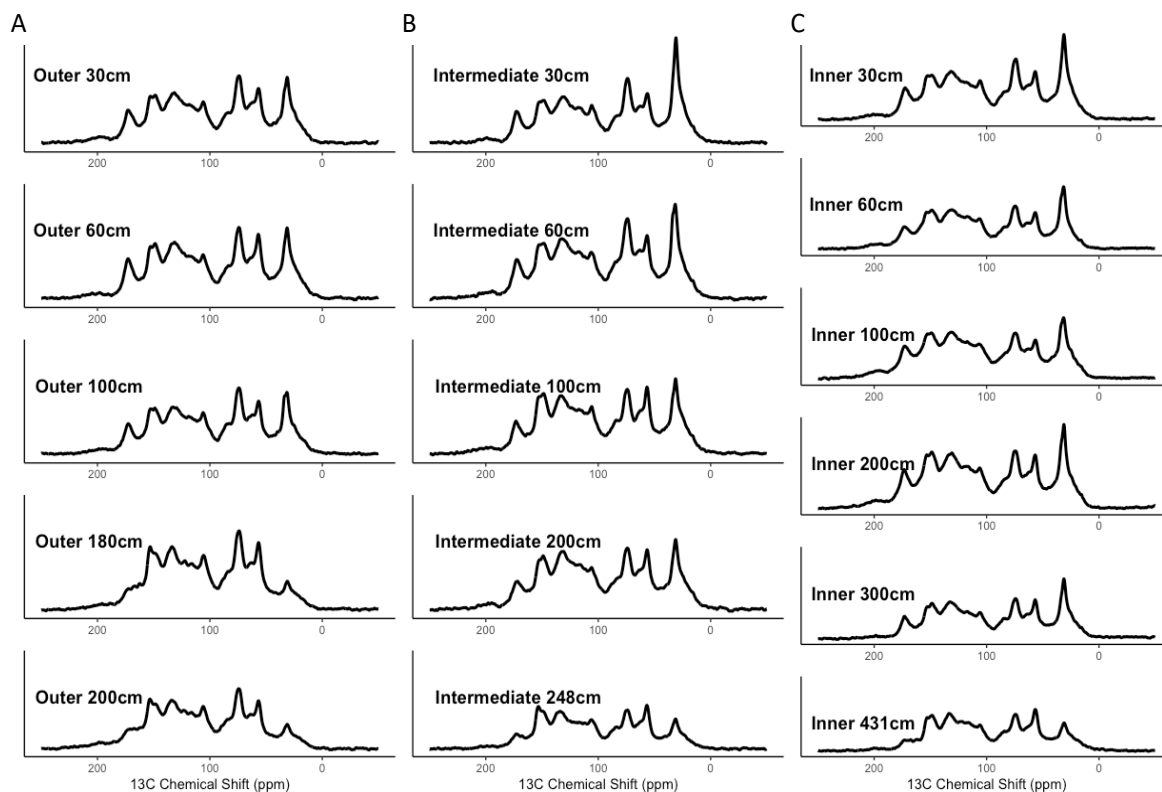
430

Fig A1



**Fig A2: Stacked overlay of depth profiles of  $^{13}\text{C}$  NMR spectra of the A) Outer, B) Intermediate, and C) Inner site. Colors increase in darkness representing an increase in depth with light green being the 30cm material and dark brown being the basal material. Spectra were digitally processed with Mnova software (v. 14.3.3; Mestrelab Research) with exponential apodization (100 Hz line broadening with the first point set to 0.50), phase correction, and baseline correction using a Bernstein polynomial fit. Peak areas were integrated corresponding to; alkyl C (0–45 ppm), N-alkyl/methoxyl C (45–60 ppm), O-alkyl C (60–95 ppm), di-O-alkyl (95–110), aromatic C (110–145 ppm), phenolic C (145–165 ppm), and carboxyl C (165–215 ppm).**

Fig A2



**Fig A3: Depth profiles of  $^{13}\text{C}$  NMR spectra for the A) Outer, B) Intermediate, and C) Inner sites. Spectra were digitally processed with Mnova software (v. 14.3.3; Mestrelab Research) with exponential apodization (100 Hz line broadening with the first point set to 0.50), phase correction, and baseline correction using a Bernstein polynomial fit. Peak areas were integrated corresponding to; alkyl C (0–45 ppm), N-alkyl/methoxyl C (45–60 ppm), O-alkyl C (60–95 ppm), di-O-alkyl (95–110), aromatic C (110–145 ppm), phenolic C (145–165 ppm), and carboxyl C (165–215 ppm). The y-axis has been scaled equally across all plots to visually compare changes in peak heights and area across depth, however the additional depths at the Inner site need to be considered when comparing across sites.**

445 **Table A3: Results from two-sample t-tests** comparing bulk peat radiocarbon values versus respiration product radiocarbon values, and DOC radiocarbon values versus respiration product radiocarbon values.

	Sample Type	Mean	t-value	df	p-value
Pair 1	Bulk Peat	-96.5625	-8.6657	15.974	1.96E-07
	Gases (CH <sub>4</sub> , CO <sub>2</sub> )	7.95			
Pair 2	DOC	2.027273	0.53811	23	0.5957
	Gases (CH <sub>4</sub> , CO <sub>2</sub> )	-3.878571			

Fig A3

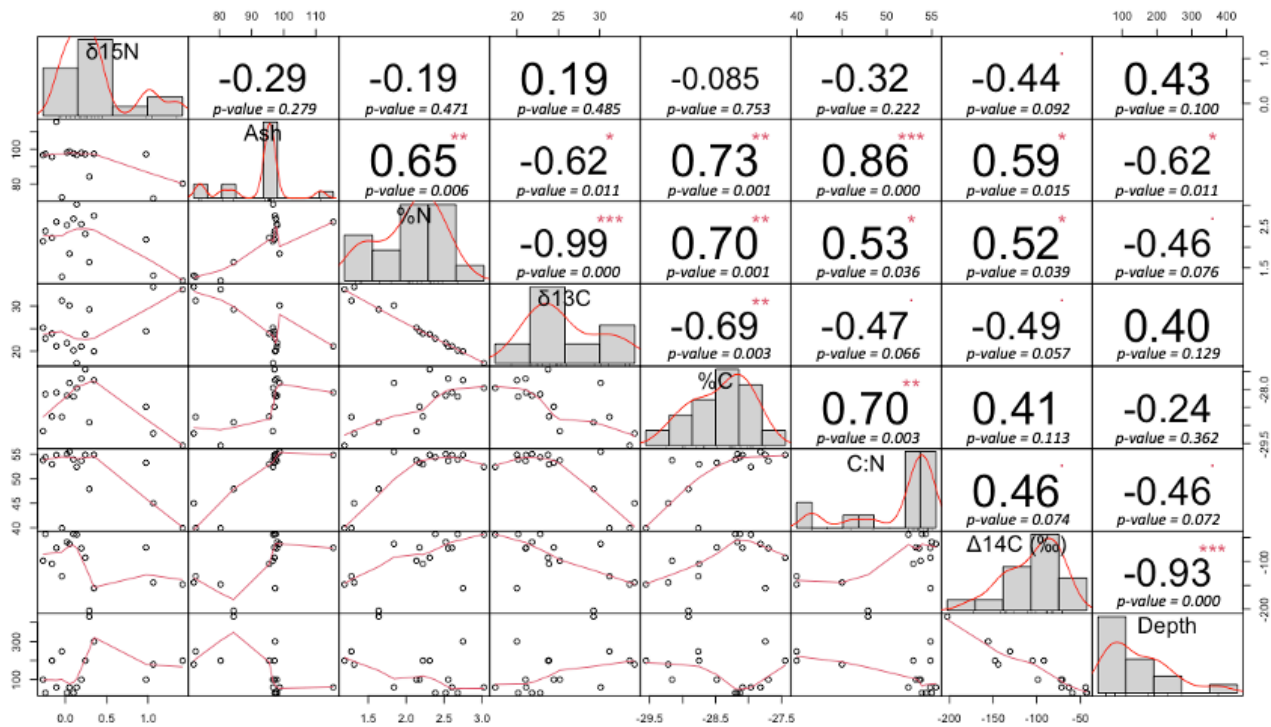
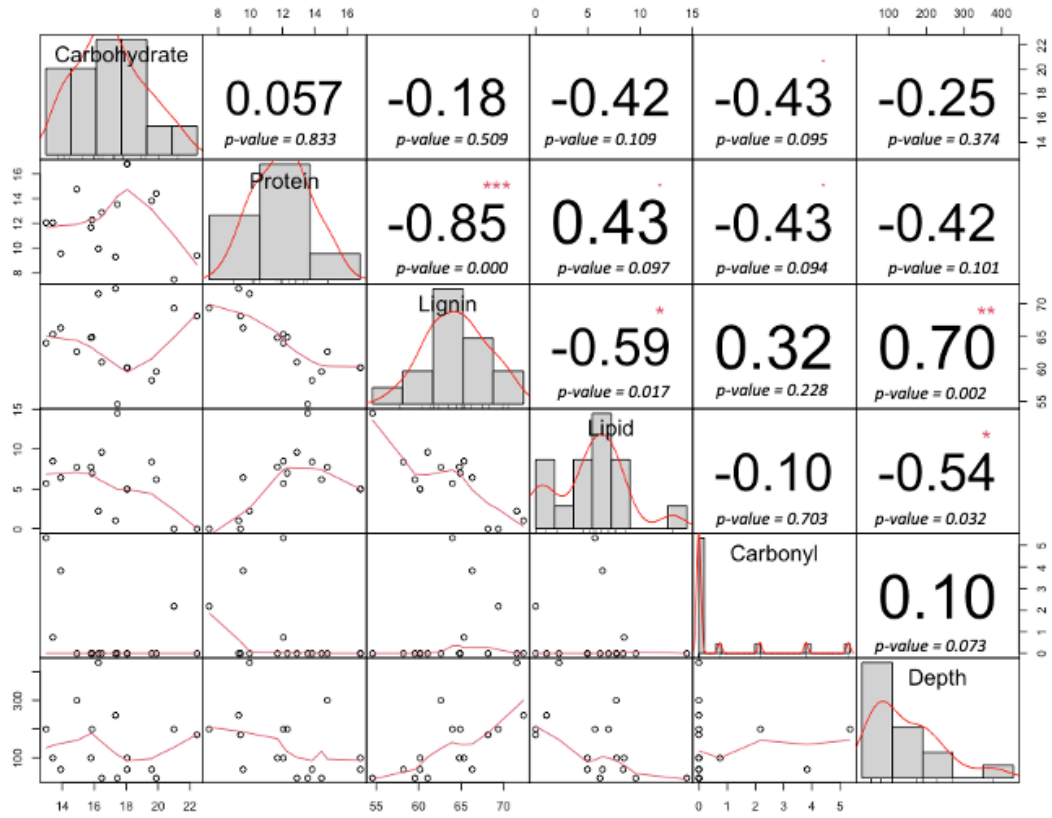


Fig A3: Correlation matrix for peat physical properties and depth. The numbers represent the value of the correlation coefficient ( $r$ ) plus the result of the cor.test as stars. On the bottom of the matrix are the bivariate scatterplots with a fitted line. Significant codes: 0 '\*\*\*' 0.001 '\*\*' 0.01 '\*' 0.1 ' '.

Fig A4

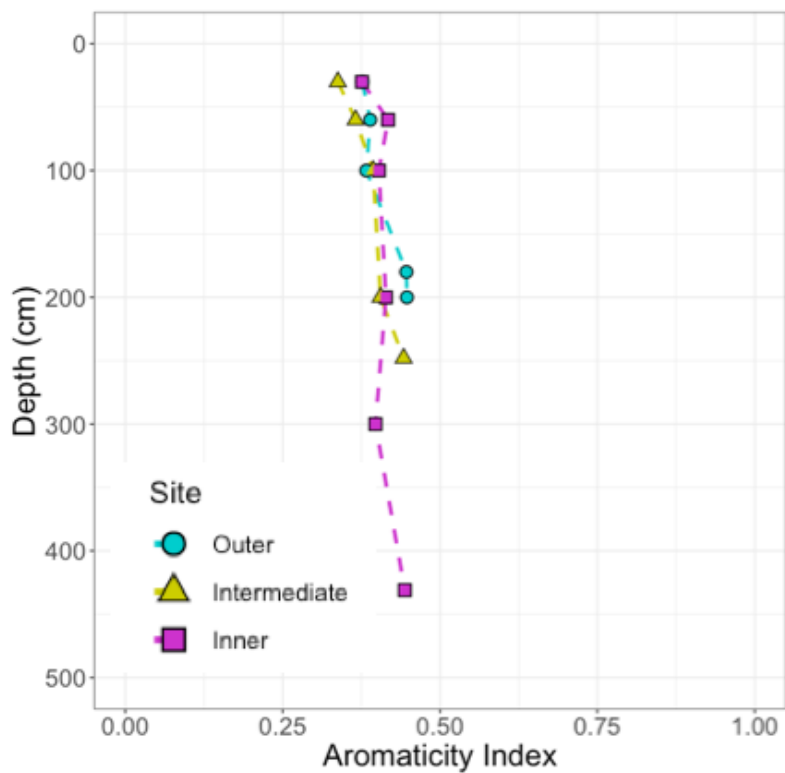


**Fig A4: Correlation matrix for peat molecular components and depth. The numbers represent the value of the correlation ( $r^2$ ) plus the result of the cor.test as stars. On the bottom of the matrix are the bivariate scatterplots with a fitted line. Significant codes: 0 '\*\*\*' 0.001 '\*\*' 0.01 '\*' 0.1 ' '.**

**Table A4:** PCA eigenvalues and loadings for PC1 and PC2.

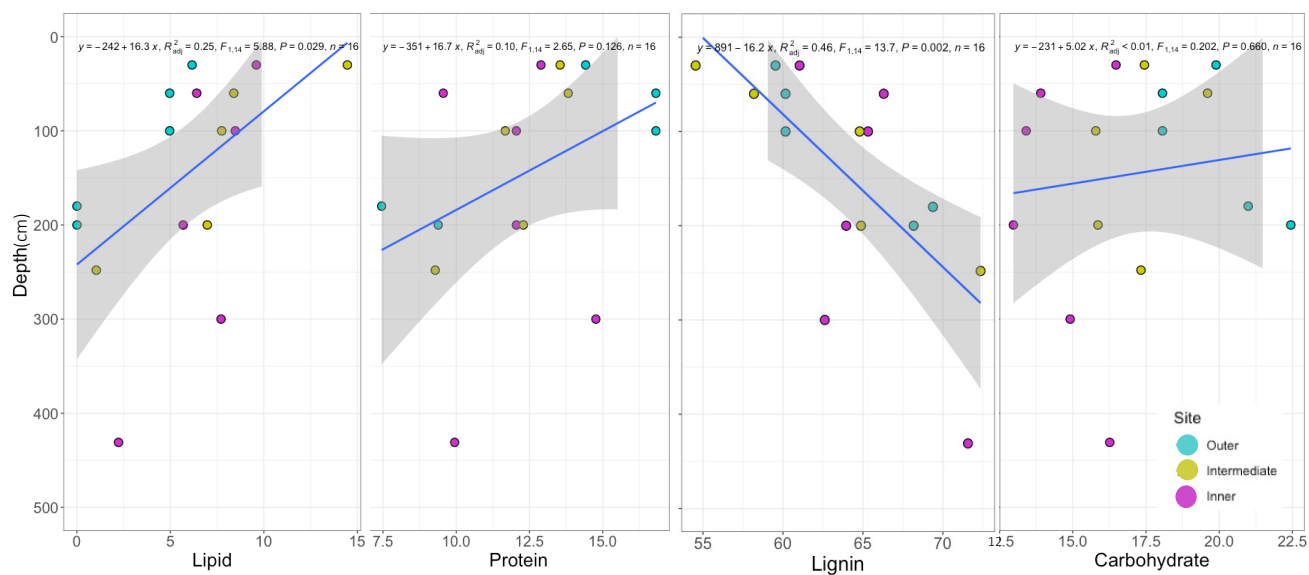
	<b>PC1</b>	<b>PC2</b>
<b>Eigenvalues</b>	<b>3.314e+00</b>	<b>1.941e+00</b>
<i>Variable</i>		
$\delta^{15}\text{N}$	-0.186	0.039
Ash	-0.386	-0.077
%N	0.274	-0.109
$\delta^{13}\text{C}$	0.230	0.165
%C	0.275	0.091
C:N	-0.266	0.144
$\Delta^{14}\text{C}$ (‰)	0.233	0.035
Depth	-0.191	0.011
LOI	0.265	-0.008
Alkyl	0.284	-0.041
N-Alkyl/Methoxyl	-0.129	-0.402
O-Alkyl	-0.156	-0.325
Di_O_Alkyl	-0.273	-0.027
Aromatic	-0.251	0.034
Phenolic	-0.230	0.296
Amide/Carboxyl	0.094	0.414
Carbohydrate	-0.121	-0.344
Protein	0.236	-0.200
Lignin	-0.264	0.157
Lipid	0.263	-0.015
Carbonyl	-0.005	0.464

Fig A5



**Fig A5: Aromaticity Index.** The aromaticity index has been used to describe decomposition state of soils. This index is expressed as the ratio of Aromatic-C to Alkyl + O-Alkyl + Aromatic C and is calculated using the results from integration of the  $^{13}\text{C}$  NMR spectra. As the aromaticity index approaches 1, the soil is considered more decomposed. The lack of change in aromaticity with depth, and the consistency across all three sites, suggests little decomposition has occurred over space and time. Sites are indicated by color and shape with blue circles indicating the outer site, yellow triangles the intermediate site, and pink squares the inner site.

Fig A6



**Fig A6: Linear regression of the four most abundant biomolecules from the mixing model versus depth. Sites have been pooled for this analysis but are indicated by color with blue indicating the outer site, yellow the intermediate site, and pink the inner site. Regressions show significant declines with depth for lipids, and significant increases with depth for lignin across sites.**

## Author Contribution

**Alexandra Hedgpeth:** Conceptualization; funding acquisition; data collection; formal analysis; investigation; methodology; visualization; writing – original draft. **Alison Hoyt:** Methodology; resources; formal analysis; visualization; supervision; writing – review and editing. **Daniela Cusack:** Conceptualization; funding acquisition; methodology; supervision; visualization; writing – review and editing. **Kyle Cavanaugh:** Supervision; writing – review and editing. **Karis McFarlane:** Funding acquisition; resources; methodology; supervision; writing – review and editing. Karis J. McFarlane and Daniela F. Cusack should be considered joint senior authors.

## Data Availability

470 Following publication, the data that supports this manuscript will be publicly available at the US Department of Energy’s Environmental Systems Science Data Infrastructure for a Virtual Ecosystem (ESS-DIVE: <https://ess-dive.lbl.gov/>) and will be submitted to the International Soil Radiocarbon Database (<https://soilradiocarbon.org/>).

## Competing interests

475 The contact author has declared that none of the authors has any competing interests.

## Acknowledgements

A. Hedgpeth thanks the Smithsonian Tropical Research Institute for a short-term research fellowship, Eric Brown for field support, and the staff at the Smithsonian Tropical Research Institute and the Bocas del Toro field station for logistical support.

480 This project was supported in part by a University of California-National Lab In-Residence Graduate Fellowship (#L21GF3629) to A. Hedgpeth, which was hosted by Lawrence Livermore National Laboratory. The <sup>13</sup>C-NMR analysis for this work was supported under a U.S. Department of Energy User Award (#60514) to D. Cusack and A. Hedgpeth, which was conducted at the Environmental Molecular Sciences Laboratory. Access to field and lab sites in Panama was supported by DOE Office of Science Early Career Award DE-SC0015898 and NSF Geography & Spatial Studies Grant #BCS-1437591 to

485 D. Cusack. We would like to thank Sarah Burton and Andrew Lipton from the Environmental Molecular Sciences Laboratory for their assistance with the <sup>13</sup>C-NMR analysis. A portion of this work was performed under the auspices of the U.S. Department of Energy by Lawrence Livermore National Laboratory under Contract DE-AC52-07NA27344 and funded by the U.S. Department of Energy Office of Science Early Career Program Award (#SCW1572) to K. McFarlane. We would like to thank Antonia L. Herwig, Lee Dietterich, and Makenna Brown for their assistance in the field.

## 490 References

Aliev, A. E.: Solid state NMR spectroscopy, in: Nuclear Magnetic Resonance, edited by: Hodgkinson, P., The Royal Society of Chemistry, 139–187, <https://doi.org/10.1039/9781788010665-00139>, 2020.

- Anderson, J. A. R. and Muller, J.: Palynological study of a holocene peat and a miocene coal deposit from NW Borneo, *Review of Palaeobotany and Palynology*, 19, 291–351, [https://doi.org/10.1016/0034-6667\(75\)90049-4](https://doi.org/10.1016/0034-6667(75)90049-4), 1975.
- 495 Aravena, R., Warner, B. G., Charman, D. J., Belyea, L. R., Mathur, S. P., and Diné, H.: Carbon Isotopic Composition of Deep Carbon Gases in an Ombrogenous Peatland, Northwestern Ontario, Canada, *Radiocarbon*, 35, 271–276, <https://doi.org/10.1017/S0033822200064948>, 1993.
- Bader, C., Müller, M., Schulin, R., and Leifeld, J.: Peat decomposability in managed organic soils in relation to land use, organic matter composition and temperature, *Biogeosciences*, 15, 703–719, <https://doi.org/10.5194/bg-15-703-2018>, 2018.
- 500 Baldock, J. A., Masiello, C. A., Gélinas, Y., and Hedges, J. I.: Cycling and composition of organic matter in terrestrial and marine ecosystems, *Marine Chemistry*, 92, 39–64, <https://doi.org/10.1016/j.marchem.2004.06.016>, 2004.
- Barreto, C. and Lindo, Z.: Decomposition in Peatlands: Who Are the Players and What Affects Them?, *Front. Young Minds*, 8, 107, <https://doi.org/10.3389/frym.2020.00107>, 2020.
- 505 Beilman, D. W., Massa, C., Nichols, J. E., Elison Timm, O., Kallstrom, R., and Dunbar-Co, S.: Dynamic Holocene Vegetation and North Pacific Hydroclimate Recorded in a Mountain Peatland, Moloka‘i, Hawai‘i, *Front. Earth Sci.*, 7, 188, <https://doi.org/10.3389/feart.2019.00188>, 2019.
- 510 Broek, T. A. B., Ognibene, T. J., McFarlane, K. J., Moreland, K. C., Brown, T. A., and Bench, G.: Conversion of the LLNL/CAMS 1 MV biomedical AMS system to a semi-automated natural abundance <sup>14</sup>C spectrometer: system optimization and performance evaluation, *Nuclear Instruments and Methods in Physics Research Section B: Beam Interactions with Materials and Atoms*, 499, 124–132, <https://doi.org/10.1016/j.nimb.2021.01.022>, 2021.
- Chanton, J. P., Glaser, P. H., Chasar, L. S., Burdige, D. J., Hines, M. E., Siegel, D. I., Tremblay, L. B., and Cooper, W. T.: Radiocarbon evidence for the importance of surface vegetation on fermentation and methanogenesis in contrasting types of boreal peatlands, *Global Biogeochemical Cycles*, 22, 2008GB003274, <https://doi.org/10.1029/2008GB003274>, 2008.
- 515 Charman, D. J., Aravena, R., Bryant, C. L., and Harkness, D. D.: Carbon isotopes in peat, DOC, CO<sub>2</sub>, and CH<sub>4</sub> in a Holocene peatland on Dartmoor, southwest England, *Geol*, 27, 539, [https://doi.org/10.1130/0091-7613\(1999\)027<0539:CIIPDC>2.3.CO;2](https://doi.org/10.1130/0091-7613(1999)027<0539:CIIPDC>2.3.CO;2), 1999.
- Chen, X., Xue, D., Wang, Y., Qiu, Q., Wu, L., Wang, M., Liu, J., and Chen, H.: Variations in the archaeal community and associated methanogenesis in peat profiles of three typical peatland types in China, *Environmental Microbiome*, 18, 48, <https://doi.org/10.1186/s40793-023-00503-y>, 2023.
- 520 Clymo, R. S., Turunen, J., and Tolonen, K.: Carbon Accumulation in Peatland, *Oikos*, 81, 368, <https://doi.org/10.2307/3547057>, 1998.
- Cobb, A. R., Hoyt, A. M., Gandois, L., Eri, J., Dommain, R., Abu Salim, K., Kai, F. M., Haji Su‘ut, N. S., and Harvey, C. F.: How temporal patterns in rainfall determine the geomorphology and carbon fluxes of tropical peatlands, *Proc. Natl. Acad. Sci. U.S.A.*, 114, <https://doi.org/10.1073/pnas.1701090114>, 2017.
- 525 Cohen, A. D., Raymond, R., Ramirez, A., Morales, Z., and Ponce, F.: The Changuinola peat deposit of northwestern Panama: a tropical, back-barrier, peat(coal)-forming environment, *International Journal of Coal Geology*, 12, 157–192, [https://doi.org/10.1016/0166-5162\(89\)90050-5](https://doi.org/10.1016/0166-5162(89)90050-5), 1989.
- Corbett, J. E.: DOC reactivity in a northern Minnesota peatland, Phd dissertation, 2012.

- 530 Corbett, J. E., Tfaily, M. M., Burdige, D. J., Cooper, W. T., Glaser, P. H., and Chanton, J. P.: Partitioning pathways of CO<sub>2</sub> production in peatlands with stable carbon isotopes, *Biogeochemistry*, 114, 327–340, <https://doi.org/10.1007/s10533-012-9813-1>, 2013.
- Dargie, G. C., Lewis, S. L., Lawson, I. T., Mitchard, E. T. A., Page, S. E., Bocko, Y. E., and Ifo, S. A.: Age, extent and carbon storage of the central Congo Basin peatland complex, *Nature*, 542, 86–90, <https://doi.org/10.1038/nature21048>, 2017.
- 535 Dhandapani, S., Girkin, N. T., and Evers, S.: Spatial variability of surface peat properties and carbon emissions in a tropical peatland oil palm monoculture during a dry season, *Soil Use and Management*, 38, 381–395, <https://doi.org/10.1111/sum.12741>, 2022.
- Dhandapani, S., Evers, S., Boyd, D., Evans, C. D., Page, S., Parish, F., and Sjögersten, S.: Assessment of differences in peat physico-chemical properties, surface subsidence and GHG emissions between the major land-uses of Selangor peatlands, *CATENA*, 230, 107255, <https://doi.org/10.1016/j.catena.2023.107255>, 2023.
- 540 Dommain, R., Cobb, A. R., Joosten, H., Glaser, P. H., Chua, A. F. L., Gandois, L., Kai, F., Noren, A., Salim, K. A., Su'ut, N. S. H., and Harvey, C. F.: Forest dynamics and tip-up pools drive pulses of high carbon accumulation rates in a tropical peat dome in Borneo (Southeast Asia), *JGR Biogeosciences*, 120, 617–640, <https://doi.org/10.1002/2014JG002796>, 2015.
- Drollinger, S., Kuzyakov, Y., and Glatzel, S.: Effects of peat decomposition on  $\delta^{13}\text{C}$  and  $\delta^{15}\text{N}$  depth profiles of Alpine bogs, *CATENA*, 178, 1–10, <https://doi.org/10.1016/j.catena.2019.02.027>, 2019.
- 545 Farmer, J., Matthews, R., Smith, J. U., Smith, P., and Singh, B. K.: Assessing existing peatland models for their applicability for modelling greenhouse gas emissions from tropical peat soils, *Current Opinion in Environmental Sustainability*, 3, 339–349, <https://doi.org/10.1016/j.cosust.2011.08.010>, 2011.
- Fritts, R.: Tropical Wetlands Emit More Methane Than Previously Thought, *Eos*, 103, <https://doi.org/10.1029/2022EO220443>, 2022.
- 550 Gandois, L., Teisserenc, R., Cobb, A. R., Chieng, H. I., Lim, L. B. L., Kamariah, A. S., Hoyt, A., and Harvey, C. F.: Origin, composition, and transformation of dissolved organic matter in tropical peatlands, *Geochimica et Cosmochimica Acta*, 137, 35–47, <https://doi.org/10.1016/j.gca.2014.03.012>, 2014.
- Girkin, N. T., Turner, B. L., Ostle, N., Craigon, J., and Sjögersten, S.: Root exudate analogues accelerate CO<sub>2</sub> and CH<sub>4</sub> production in tropical peat, *Soil Biology and Biochemistry*, 117, 48–55, <https://doi.org/10.1016/j.soilbio.2017.11.008>, 2018.
- 555 Girkin, N. T., Vane, C. H., Cooper, H. V., Moss-Hayes, V., Craigon, J., Turner, B. L., Ostle, N., and Sjögersten, S.: Spatial variability of organic matter properties determines methane fluxes in a tropical forested peatland, *Biogeochemistry*, 142, 231–245, <https://doi.org/10.1007/s10533-018-0531-1>, 2019.
- Girkin, N. T., Dhandapani, S., Evers, S., Ostle, N., Turner, B. L., and Sjögersten, S.: Interactions between labile carbon, temperature and land use regulate carbon dioxide and methane production in tropical peat, *Biogeochemistry*, 147, 87–97, <https://doi.org/10.1007/s10533-019-00632-y>, 2020.
- 560 Girkin, N. T., Cooper, H. V., Ledger, M. J., O'Reilly, P., Thornton, S. A., Åkesson, C. M., Cole, L. E. S., Hapsari, K. A., Hawthorne, D., and Roucoux, K. H.: Tropical peatlands in the Anthropocene: The present and the future, *Anthropocene*, 40, 100354, <https://doi.org/10.1016/j.ancene.2022.100354>, 2022.
- 565 Goldstein, A., Turner, W. R., Spawn, S. A., Anderson-Teixeira, K. J., Cook-Patton, S., Fargione, J., Gibbs, H. K., Griscom, B., Hewson, J. H., Howard, J. F., Ledezma, J. C., Page, S., Koh, L. P., Rockström, J., Sanderman, J., and Hole, D. G.: Protecting

- irrecoverable carbon in Earth's ecosystems, *Nat. Clim. Chang.*, 10, 287–295, <https://doi.org/10.1038/s41558-020-0738-8>, 2020.
- Gruca-Rokosz, R. and Koszelnik, P.: Production pathways for CH<sub>4</sub> and CO<sub>2</sub> in sediments of two freshwater ecosystems in south-eastern Poland, *PLoS ONE*, 13, e0199755, <https://doi.org/10.1371/journal.pone.0199755>, 2018.
- 570 Hirano, T., Jauhiainen, J., Inoue, T., and Takahashi, H.: Controls on the Carbon Balance of Tropical Peatlands, *Ecosystems*, 12, 873–887, <https://doi.org/10.1007/s10021-008-9209-1>, 2009.
- Hobbie, E. A. and Ouimette, A. P.: Controls of nitrogen isotope patterns in soil profiles, *Biogeochemistry*, 95, 355–371, <https://doi.org/10.1007/s10533-009-9328-6>, 2009.
- 575 Hodgkins, S. B., Richardson, C. J., Dommain, R., Wang, H., Glaser, P. H., Verbeke, B., Winkler, B. R., Cobb, A. R., Rich, V. I., Missilmani, M., Flanagan, N., Ho, M., Hoyt, A. M., Harvey, C. F., Vining, S. R., Hough, M. A., Moore, T. R., Richard, P. J. H., De La Cruz, F. B., Toufaily, J., Hamdan, R., Cooper, W. T., and Chanton, J. P.: Tropical peatland carbon storage linked to global latitudinal trends in peat recalcitrance, *Nat Commun*, 9, 3640, <https://doi.org/10.1038/s41467-018-06050-2>, 2018.
- 580 Hornibrook, E. R. C., Longstaffe, F. J., and Fyfe, W. S.: Evolution of stable carbon isotope compositions for methane and carbon dioxide in freshwater wetlands and other anaerobic environments, *Geochimica et Cosmochimica Acta*, 64, 1013–1027, [https://doi.org/10.1016/S0016-7037\(99\)00321-X](https://doi.org/10.1016/S0016-7037(99)00321-X), 2000a.
- Hornibrook, E. R. C., Longstaffe, F. J., and Fyfe, W. S.: Factors Influencing Stable Isotope Ratios in CH<sub>4</sub> and CO<sub>2</sub> Within Subenvironments of Freshwater Wetlands: Implications for δ-Signatures of Emissions, *Isotopes in Environmental and Health Studies*, 36, 151–176, <https://doi.org/10.1080/10256010008032940>, 2000b.
- 585 Hoyos-Santillan, J.: 2014 Hoyos Controls of Carbon Turnover in Tropical Peatlands, <https://doi.org/10.13140/2.1.3387.2329>, 2014.
- Hoyos-Santillan, J., Lomax, B. H., Large, D., Turner, B. L., Boom, A., Lopez, O. R., and Sjögersten, S.: Quality not quantity: Organic matter composition controls of CO<sub>2</sub> and CH<sub>4</sub> fluxes in neotropical peat profiles, *Soil Biology and Biochemistry*, 103, 86–96, <https://doi.org/10.1016/j.soilbio.2016.08.017>, 2016.
- 590 Hoyos-Santillan, J., Lomax, B. H., Large, D., Turner, B. L., Lopez, O. R., Boom, A., Sepulveda-Jauregui, A., and Sjögersten, S.: Evaluation of vegetation communities, water table, and peat composition as drivers of greenhouse gas emissions in lowland tropical peatlands, *Science of The Total Environment*, 688, 1193–1204, <https://doi.org/10.1016/j.scitotenv.2019.06.366>, 2019.
- Hoyt, A.: Methane production and transport in a tropical peatland, *AGU Fall Meeting Abstracts*, 2014.
- 595 Hoyt, A., Cadillo-Quiroz, H., Xu, X., Torn, M., Bazán Pacaya, A., Jacobs, M., Shapiama Peña, R., Ramirez Navarro, D., Urquiza-Muñoz, D., and Trumbore, S.: Isotopic Insights into Methane Production and Emission in Diverse Amazonian Peatlands, oral, <https://doi.org/10.5194/egusphere-egu2020-12960>, 2020.
- Hoyt, A. M., Gandois, L., Eri, J., Kai, F. M., Harvey, C. F., and Cobb, A. R.: CO<sub>2</sub> emissions from an undrained tropical peatland: Interacting influences of temperature, shading and water table depth, *Global Change Biology*, 25, 2885–2899, <https://doi.org/10.1111/gcb.14702>, 2019.
- 600 Ingram, H. A. P.: Ecohydrology of Scottish peatlands, *Transactions of the Royal Society of Edinburgh: Earth Sciences*, 78, 287–296, <https://doi.org/10.1017/S0263593300011226>, 1987.

- Jauhiainen, J., Takahashi, H., Heikkinen, J. E. P., Martikainen, P. J., and Vasander, H.: Carbon fluxes from a tropical peat swamp forest floor, *Global Change Biology*, 11, 1788–1797, <https://doi.org/10.1111/j.1365-2486.2005.001031.x>, 2005.
- Kettridge, N., Turetsky, M. R., Sherwood, J. H., Thompson, D. K., Miller, C. A., Benschoter, B. W., Flannigan, M. D., Wotton, B. M., and Waddington, J. M.: Moderate drop in water table increases peatland vulnerability to post-fire regime shift, *Sci Rep*, 5, 8063, <https://doi.org/10.1038/srep08063>, 2015.
- Kotsyurbenko, O. R., Chin, K.-J., Glagolev, M. V., Stubner, S., Simankova, M. V., Nozhevnikova, A. N., and Conrad, R.: Acetoclastic and hydrogenotrophic methane production and methanogenic populations in an acidic West-Siberian peat bog, *Environ Microbiol*, 6, 1159–1173, <https://doi.org/10.1111/j.1462-2920.2004.00634.x>, 2004.
- Lähteenoja, O., Reátegui, Y. R., Räsänen, M., Torres, D. D. C., Oinonen, M., and Page, S.: The large Amazonian peatland carbon sink in the subsiding Parana-Paraguay foreland basin, *Global Change Biology*, 18, 164–178, <https://doi.org/10.1111/j.1365-2486.2011.02504.x>, 2012.
- Lampela, M., Jauhiainen, J., and Vasander, H.: Surface peat structure and chemistry in a tropical peat swamp forest, *Plant Soil*, 382, 329–347, <https://doi.org/10.1007/s11104-014-2187-5>, 2014.
- Ledru, M.-P., Braga, P. I. S., Soubiès, F., Fournier, M., Martin, L., Suguio, K., and Turcq, B.: The last 50,000 years in the Neotropics (Southern Brazil): evolution of vegetation and climate, *Palaeogeography, Palaeoclimatology, Palaeoecology*, 123, 239–257, [https://doi.org/10.1016/0031-0182\(96\)00105-8](https://doi.org/10.1016/0031-0182(96)00105-8), 1996.
- Li, D., Ni, H., Jiao, S., Lu, Y., Zhou, J., Sun, B., and Liang, Y.: Coexistence patterns of soil methanogens are closely tied to methane generation and community assembly in rice paddies, *Microbiome*, 9, 20, <https://doi.org/10.1186/s40168-020-00978-8>, 2021.
- Liebner, S., Ganzert, L., Kiss, A., Yang, S., Wagner, D., and Svenning, M. M.: Shifts in methanogenic community composition and methane fluxes along the degradation of discontinuous permafrost, *Front. Microbiol.*, 6, <https://doi.org/10.3389/fmicb.2015.00356>, 2015.
- Loisel, J., Gallego-Sala, A. V., Amesbury, M. J., Magnan, G., Anshari, G., Beilman, D. W., Benavides, J. C., Blewett, J., Camill, P., Charman, D. J., Chawchai, S., Hedgpeth, A., Kleinen, T., Korhola, A., Large, D., Mansilla, C. A., Müller, J., Van Bellen, S., West, J. B., Yu, Z., Bubier, J. L., Garneau, M., Moore, T., Sannel, A. B. K., Page, S., Väliranta, M., Bechtold, M., Brovkin, V., Cole, L. E. S., Chanton, J. P., Christensen, T. R., Davies, M. A., De Vleeschouwer, F., Finkelstein, S. A., Frolking, S., Gałka, M., Gandois, L., Girkin, N., Harris, L. I., Heinemeyer, A., Hoyt, A. M., Jones, M. C., Joos, F., Juutinen, S., Kaiser, K., Lacourse, T., Lamentowicz, M., Larmola, T., Leifeld, J., Lohila, A., Milner, A. M., Minkinen, K., Moss, P., Naafs, B. D. A., Nichols, J., O'Donnell, J., Payne, R., Philben, M., Piilo, S., Quillet, A., Ratnayake, A. S., Roland, T. P., Sjögersten, S., Sonntag, O., Swindles, G. T., Swinnen, W., Talbot, J., Treat, C., Valach, A. C., and Wu, J.: Expert assessment of future vulnerability of the global peatland carbon sink, *Nat. Clim. Chang.*, 11, 70–77, <https://doi.org/10.1038/s41558-020-00944-0>, 2021.
- Malmer, N. and Holm, E.: Variation in the C/N-Quotient of Peat in Relation to Decomposition Rate and Age Determination with <sup>210</sup>Pb, *Oikos*, 43, 171, <https://doi.org/10.2307/3544766>, 1984.
- McNicol, G., Knox, S. H., Guilderson, T. P., Baldocchi, D. D., and Silver, W. L.: Where old meets new: An ecosystem study of methanogenesis in a reflooded agricultural peatland, *Global Change Biology*, 26, 772–785, <https://doi.org/10.1111/gcb.14916>, 2020.

- 640 Noon, M. L., Goldstein, A., Ledezma, J. C., Roehrdanz, P. R., Cook-Patton, S. C., Spawn-Lee, S. A., Wright, T. M., Gonzalez-Roglich, M., Hole, D. G., Rockström, J., and Turner, W. R.: Mapping the irrecoverable carbon in Earth's ecosystems, *Nat Sustain*, 5, 37–46, <https://doi.org/10.1038/s41893-021-00803-6>, 2021.
- Norris, M. W., Turnbull, J. C., Howarth, J. D., and Vandergoes, M. J.: Pretreatment of Terrestrial Macrofossils, *Radiocarbon*, 62, 349–360, <https://doi.org/10.1017/RDC.2020.8>, 2020.
- 645 Nottingham, A. T., Bååth, E., Reischke, S., Salinas, N., and Meir, P.: Adaptation of soil microbial growth to temperature: Using a tropical elevation gradient to predict future changes, *Global Change Biology*, 25, 827–838, <https://doi.org/10.1111/gcb.14502>, 2019.
- Ofiti, N. O. E., Schmidt, M. W. I., Abiven, S., Hanson, P. J., Iversen, C. M., Wilson, R. M., Kostka, J. E., Wiesenberg, G. L. B., and Malhotra, A.: Climate warming and elevated CO<sub>2</sub> alter peatland soil carbon sources and stability, *Nat Commun*, 14, 7533, <https://doi.org/10.1038/s41467-023-43410-z>, 2023.
- 650 Omar, M. S., Ifandi, E., Sukri, R. S., Kalaitzidis, S., Christanis, K., Lai, D. T. C., Bashir, S., and Tsikouras, B.: Peatlands in Southeast Asia: A comprehensive geological review, *Earth-Science Reviews*, 232, 104149, <https://doi.org/10.1016/j.earscirev.2022.104149>, 2022.
- Osaki, M., Kato, T., Kohyama, T., Takahashi, H., Haraguchi, A., Yabe, K., Tsuji, N., Shiodera, S., Rahajoe, J. S., Atikah, T. D., Oide, A., Matsui, K., Wetadewi, R. I., and Silsigia, S.: Basic Information About Tropical Peatland Ecosystems, in: *Tropical Peatland Eco-management*, edited by: Osaki, M., Tsuji, N., Focad, N., and Rieley, J., Springer Singapore, Singapore, 3–62, [https://doi.org/10.1007/978-981-33-4654-3\\_1](https://doi.org/10.1007/978-981-33-4654-3_1), 2021.
- 655 Page, S. E., Rieley, J. O., and Banks, C. J.: Global and regional importance of the tropical peatland carbon pool, *Global Change Biology*, 17, 798–818, <https://doi.org/10.1111/j.1365-2486.2010.02279.x>, 2011.
- Phillips, S. and Bustin, R. M.: Sedimentology of the Changuinola peat deposit: Organic and clastic sedimentary response to punctuated coastal subsidence, *Geological Society of America Bulletin*, 108, 794–814, [https://doi.org/10.1130/0016-7606\(1996\)108<0794:SOTCPD>2.3.CO;2](https://doi.org/10.1130/0016-7606(1996)108<0794:SOTCPD>2.3.CO;2), 1996.
- 660 Phillips, S., Rouse, G. E., and Bustin, R. M.: Vegetation zones and diagnostic pollen profiles of a coastal peat swamp, *Bocas del Toro, Panamá, Palaeogeography, Palaeoclimatology, Palaeoecology*, 128, 301–338, [https://doi.org/10.1016/S0031-0182\(97\)81129-7](https://doi.org/10.1016/S0031-0182(97)81129-7), 1997.
- Ribeiro, K., Pacheco, F. S., Ferreira, J. W., De Sousa-Neto, E. R., Hastie, A., Krieger Filho, G. C., Alvalá, P. C., Forti, M. C., and Ometto, J. P.: Tropical peatlands and their contribution to the global carbon cycle and climate change, *Global Change Biology*, 27, 489–505, <https://doi.org/10.1111/gcb.15408>, 2021.
- 665 Ruwaimana, M., Anshari, G. Z., Silva, L. C. R., and Gavin, D. G.: The oldest extant tropical peatland in the world: a major carbon reservoir for at least 47 000 years, *Environ. Res. Lett.*, 15, 114027, <https://doi.org/10.1088/1748-9326/abb853>, 2020.
- 670 Sihi, D., Inglett, P. W., and Inglett, K. S.: Carbon quality and nutrient status drive the temperature sensitivity of organic matter decomposition in subtropical peat soils, *Biogeochemistry*, 131, 103–119, <https://doi.org/10.1007/s10533-016-0267-8>, 2016.
- Sjögersten, S., Cheesman, A. W., Lopez, O., and Turner, B. L.: Biogeochemical processes along a nutrient gradient in a tropical ombrotrophic peatland, *Biogeochemistry*, 104, 147–163, <https://doi.org/10.1007/s10533-010-9493-7>, 2011.
- Sugimoto, A. and Wada, E.: Carbon isotopic composition of bacterial methane in a soil incubation experiment: Contributions of acetate and, *Geochimica et Cosmochimica Acta*, 57, 4015–4027, [https://doi.org/10.1016/0016-7037\(93\)90350-6](https://doi.org/10.1016/0016-7037(93)90350-6), 1993.

- 675 Sun, C. L., Brauer, S. L., Cadillo-Quiroz, H., Zinder, S. H., and Yavitt, J. B.: Seasonal Changes in Methanogenesis and Methanogenic Community in Three Peatlands, New York State, *Front. Microbio.*, 3, <https://doi.org/10.3389/fmicb.2012.00081>, 2012.
- Troxler, T. G.: Patterns of phosphorus, nitrogen and  $\delta^{15}\text{N}$  along a peat development gradient in a coastal mire, Panama, *J. Trop. Ecol.*, 23, 683–691, <https://doi.org/10.1017/S0266467407004464>, 2007.
- 680 Troxler, T. G., Ikenaga, M., Scinto, L., Boyer, J. N., Condit, R., Perez, R., Gann, G. D., and Childers, D. L.: Patterns of Soil Bacteria and Canopy Community Structure Related to Tropical Peatland Development, *Wetlands*, 32, 769–782, <https://doi.org/10.1007/s13157-012-0310-z>, 2012.
- United Nations Environment Programme, Global Environment Facility, Asia Pacific Network for Global Change Research, Global Environment Centre (Malaysia), and Wetlands International (Eds.): Assessment on peatlands, biodiversity, and climate change, Global Environment Centre & Wetlands International, Wageningen, Kuala Lumpur, 2 pp., 2008.
- 685
- Upton, A., Vane, C. H., Girkin, N., Turner, B. L., and Sjögersten, S.: Does litter input determine carbon storage and peat organic chemistry in tropical peatlands?, *Geoderma*, 326, 76–87, <https://doi.org/10.1016/j.geoderma.2018.03.030>, 2018.
- Wilson, R. M., Hopple, A. M., Tfaily, M. M., Sebestyén, S. D., Schadt, C. W., Pfeifer-Meister, L., Medvedeff, C., McFarlane, K. J., Kostka, J. E., Kolton, M., Kolka, R. K., Kluber, L. A., Keller, J. K., Guilderson, T. P., Griffiths, N. A., Chanton, J. P.,
- 690 Bridgham, S. D., and Hanson, P. J.: Stability of peatland carbon to rising temperatures, *Nat Commun*, 7, 13723, <https://doi.org/10.1038/ncomms13723>, 2016.
- Wilson, R. M., Griffiths, N. A., Visser, A., McFarlane, K. J., Sebestyén, S. D., Oleheiser, K. C., Bosman, S., Hopple, A. M., Tfaily, M. M., Kolka, R. K., Hanson, P. J., Kostka, J. E., Bridgham, S. D., Keller, J. K., and Chanton, J. P.: Radiocarbon Analyses Quantify Peat Carbon Losses With Increasing Temperature in a Whole Ecosystem Warming Experiment, *JGR Biogeosciences*, 126, e2021JG006511, <https://doi.org/10.1029/2021JG006511>, 2021.
- 695
- Wright, E. L., Black, C. R., Cheesman, A. W., Drage, T., Large, D., Turner, B. L., and Sjögersten, S.: Contribution of subsurface peat to CO<sub>2</sub> and CH<sub>4</sub> fluxes in a neotropical peatland: CARBON FLUXES IN A NEOTROPICAL PEATLAND, *Global Change Biology*, 17, 2867–2881, <https://doi.org/10.1111/j.1365-2486.2011.02448.x>, 2011.
- Wright, E. L., Black, C. R., Turner, B. L., and Sjögersten, S.: Environmental controls of temporal and spatial variability in
- 700 CO<sub>2</sub> and CH<sub>4</sub> fluxes in a neotropical peatland, *Global Change Biology*, 19, 3775–3789, <https://doi.org/10.1111/gcb.12330>, 2013.
- Zhang, Y., Ma, A., Zhuang, G., and Zhuang, X.: The acetotrophic pathway dominates methane production in Zoige alpine wetland coexisting with hydrogenotrophic pathway, *Sci Rep*, 9, 9141, <https://doi.org/10.1038/s41598-019-45590-5>, 2019.